Rechargeable Sodium Aqueous Batteries

Novel Polymer Anodes

Alexander Selz

in order to fulfill the requirements for the degree

Master of Science
Sustainable Energy Technology

at Delft University of Technology

Storage of Electrochemical Energy

Reactor Instituut Delft

Faculty of Electrical Engineering, Mathematics, and Computer Science

Delft University of Technology

Student Number: 4590074

Supervisor:	Dr. ir. M. Wagemaker	TU Delft
Daily Supervisor:	Ir. R. van der Jagt	TU Delft
Thesis Committee:	Dr. ir. M. Wagemaker	TU Delft
	Dr. ir. E. Kelder	TU Delft
	Prof. dr. ir. S. Picken	TU Delft

TU Delft

REACTOR INSTITUTE DELFT

Abstract

Due to the increasing need for large scale energy storage batteries have become a subject of great interest. Sodium aqueous batteries have the potential to deliver the kind of affordable grid scale energy storage needed to assist renewables penetration and power/price stability in the market. Since there are several well known positive electrodes available, more focus is dedicated so finding suitable negative electrodes for aqueous cells. Here we investigated polymer anodes due to their use of abundant elements, good performance, facile synthesis, and insolubility in aqueous electrolytes. Of the three base compounds chosen (anthraquinone, naphthalene diimide, and naphthalimide) only naphthalimide was successfully polymerized. However, the yield was small so the recovered monomers were tested instead. As a result, solubility issues were encountered in organic cell testing as expected, but in the end it was possible to make a fully reversible naphthalene diimide based cell with sodium manganese oxide as the positive electrode. The naphthalene diimide was not soluble in aqueous electrolyte and seemed to display optimistic results, so given the right choice of organic material polymerization may be unnecessary and these compounds seem promising for delivering reliable capacities affordably at a large scale.

Table of Contents:

1 Introduction

Since the industrial revolution our planet has seen drastic changes in all aspects of our society. Our population is growing, our standards of living rising, and consumption per capita reaching new highs. All of these factors share a common denominator being increased energy usage. While fossil fuels have undeniably been one of the most robust and cheap sources of energy they are not a long term solution to our worlds growing energy needs. Furthermore, fossil fuels are attributed to many large scale environmental problems, such as pollution and climate change. Meanwhile the growing renewable energy market is beginning to become more cost competitive while offering environmentally friendly solutions.

A major benefit of renewable energies is that they have the potential to supply amounts of power orders of magnitude higher than what we demand for years to come. However, even as sustainable energy options become more prevalent and inexpensive they come with their own challenges. By nature of being sustainable all the energy sources derive power from natural phenomena, thus making them dependent on the environment. As weather patterns and shifts in seasons can greatly change they equally influence the power output and economics of such energy sources. These fluctuations do not coincide with the times when society requires power. Power is also unique in that supply and demand of electricity must always be perfectly matched. So while gas and oil plants can easily ramp up and down to match demand, renewable energy sources are much more limited in this regard. Therefore, energy storage is a very promising way to address the fallbacks of renewable energy as it facilities a means to store energy and save it for later usage either when demand spikes or renewable plants are producing insufficient power [11].

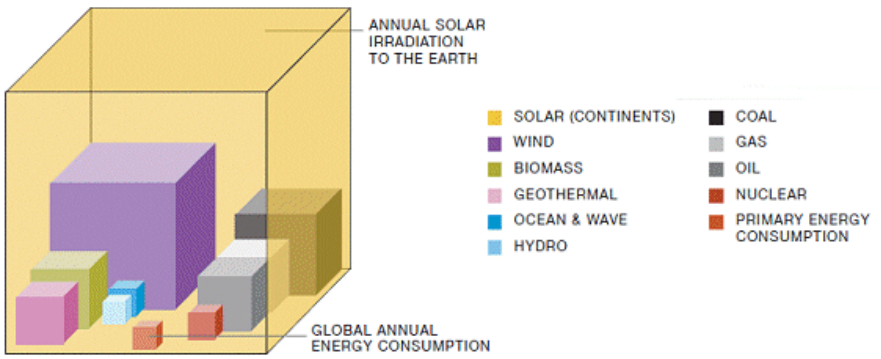

Figure 1: Estimate of potential energy reserves by different sources compared to consumption [11]

Large scale energy storage combined with renewables seems to be the long term solution. Solar panels or wind farms alone cannot address the problem. Large scale energy storage is not new. Hydro storage is one of the oldest and most common forms of energy storage [10]. It is widely used to support existing power plants with typical round trip efficiencies of roughly 80% [8]. Nevertheless, plenty of alternatives are available and attracting a lot of research attention and investment, such as flywheels, super capacitors, molten salt, and chemical storage (eg. hydrogen and nitrogen). Among the various forms of energy storage on the market, electrochemical energy storage in the form of batteries has come to the forefront as material costs have decreased and technological advancements have increased energy density, efficiency, reliability, and safety.

1.1 Battery Storage

Batteries have gotten an immense amount of attention for a variety of reasons. They have high efficiencies, high energy densities, high power densities, and decreasing costs as of lately. Lithium ion batteries have found their way into an ever increasing number of appliances and devices ranging from cell phones to cars. due to their reliability and long lifespan. Currently commercial lithium batteries have reached energy densities of 250 Wh/kg and prices of 200 €/kWh with many still aiming to reach 100 €/kWh as this is widely considered the point at which batteries are economically superior to alternatives [28].

Although lithium ion batteries have made great strides for energy storage field, difficulties still remain. Firstly, lithium is not a highly abundant element and it is mostly mined in the Argentina, Chile, and Bolivia, now known as the Lithium Triangle. As this region is rather politically unstable it poses risks it terms of consistent lithium output and stable prices. Cobalt, another common element used in lithium batteries mostly comes from the Congo which has been known for using child labor. Secondly, lithium organic batteries contain toxic, flammable, and expensive materials. These materials have made possible the compact and powerful batteries in our everyday devices, but are less desirable for the large scale stationary storage that could facilitate the energy transition from gas and oil to renewables. For such grid scale applications price, safety, and reliability become far more important factors than size and weight. Thirdly, most rechargeable Li-ion batteries also maintain high prices because production is expensive as it often requires an oxygen and water free atmosphere. While Li-ion technology has made impressive strides in recent years it still faces many challenges, especially for large scale applications [39].

There are alternative chemistries though. Lithium certainly remains at the forefront, but within the field of battery storage there are many other possible chemistries available. For example, most automobiles still contain lead-acid batteries. Zinc, vanadium, and magnesium-ion batteries are all chemistries currently being investigated; some at research level and others at a commercial scale [42].

1.2 Sodium Aqueous Batteries

One of the most promising chemistries is sodium-ion batteries. Sodium ions have a similar behavior to lithium ions as alkali metals have an urge to donate an electron spontaneously, which means that the reduction potentials can be quite low. While the radius is larger (by 24%) than that of lithium it has been shown to intercalate into many of the same materials used for lithium batteries. More importantly, sodium is the sixth most abundant element in world and its occurrence is distributed rather evenly throughout the earth's crust [26]. Many of the problems with lithium listed above have also played a role in pushing research in this direction as sodium does not face similar challenges. Sodium does have its own set of problems to overcome.

A large portion of sodium battery research is focused on organic electrolytes as they have a much wider stability window allowing for a wider and higher voltage range compared to aqueous cells. The downside to organic electrolytes is that they require oxygen and moisture free assembly environments and they can often be toxic and flammable. For these reasons aqueous electrolytes have become a topic of interest. Aqueous batteries simply use water with a dissolved sodium based salt as the electrolyte, which drastically reduces costs. One of the key features is that aqueous electrolytes are intrinsically safe and can be assembled in an open atmosphere. One of the continual issues with aqueous cells is that liquid water splits into

gaseous oxygen and hydrogen at 1.23 V. Splitting water during battery operation can cause explosion risks and accelerated degradation of the battery components. Free oxygen can bond with sodium reducing the electrolyte and inhibit functionality. However, simple and low cost solutions can prevent this, so it is not a highly relevant issue. The possibility of making cheap and safe batteries for large scale stationary energy storage make this topic attractive.

There are currently several options for cathodes in sodium aqueous batteries, yet finding suitable anodes remains difficult. In aqueous cells it is not possible to simply use pure sodium metal as a counterelectrode as sodium reacts with water, so it is necessary find materials which can host sodium ions. Problems with previously investigated materials include spontaneous oxidation of the anode, competing H^+ intercalation reactions, and dissolution of the anode into the electrolyte. There are some materials that have shown potential, such as naphthalene diimides and related organic polymers [29][41]. One of the great advantages to organic materials is that they do not contain rare or toxic materials. Additionally, they are usually very cheap.

1.3 Research Objectives

The main objective of this project was to assess the feasibility of new anode materials in a sodium aqueous full cell. This overarching goal would require breaking the project down into several key sub steps. Firstly, we would search for new materials that had sufficient capacities, proven performance (either in Na half cells or vs Li), and most importantly were functional inside the stability window of water. Then all the identified materials would be tested in organic half cells to verify their performance. Next organic full cells could be tested. Lastly, if everything thus far had gone well the same materials would be tested in aqueous full cells.

1. Research new anode materials
2. Test materials in organic half cells
3. Test organic full cells
4. Test aqueous full cells
5. Assess results and identify underlying principles that either caused certain cells to work or others to fail

This seems rather straightforward, but in reality there is a lot more to it. As is the norm with research, things will go wrong and not work. Being able to identify problems and figure out which mechanisms are responsible was the most vital aspect of the project. It is not something done at a certain point in time, but rather a mindset and approach that is systemically applied throughout. In doing so, ideally, a new and improved sodium aqueous battery can be made while gaining insight into the deeper electrochemical workings of the cell.

1.4 Report Structure

The structure of the thesis is designed to make evident a clear logic and line of thought. In this way it should be possible to see the progression of research and the motivating choices behind every decision. To accommodate this structure it begins with a chapter dedicated to theory and basic concepts necessary to move forward. Then in chapter 3 the material choices are justified. The following chapter explains the syntheses of said materials. The fifth chapter then details the results and gives some preliminary thoughts. In the last chapter conclusions are drawn based on the experimental work and recommendations for future research on the topic are offered.

2 Theoretical Background

Here the basic concepts of a functional battery are discussed. Key components of a battery are explained in order to provide the basic understanding for the rest of the report. Then an in depth view of the aspects of an aqueous electrolyte are provided. The difference between an organic and aqueous electrolyte are given along with a brief discussion of their pros and cons. Due to the nature of water a stability window for potentials is then defined for the aqueous electrolyte. In the last section certain selection criteria for the active materials are added as an aid in the selection process and to ensure they have the desired attributes for the project.

2.1 Battery Basics

The basic concept behind an electrochemical battery is the conversion of stored chemical energy into usable electrical energy. Doing the opposite then charges the battery giving it power to use at a later point in time. The release of energy comes from bonded alkali atoms becoming cations and releasing free electrons. Conversely the storage of energy is the recombination of ions and electrons in the electrode. The complete reaction comprises of two half cell reactions, one at each electrode. To satisfy the law of conservation of charge the reactions must happen simultaneously. When discharging the battery, the spontaneous reaction is driven by the potential difference between the electrodes allows power to be delivered to an external circuit. When charging, the reactions are non-spontaneous ($\Delta G>0$), so there is a need for a driving force which comes from an external applied potential between the electrodes. The generalized reaction can be written as shown in Equation 1 where Me could be a metal like lithium or sodium.

The primary components of a battery are the electrodes and electrolyte. The two electrodes are a negative anode and a positive cathode. The electrodes contain an active material, meaning that the material is capable of storing and releasing sodium ions (intercalation). Each sodium ion desorbed into the electrolyte is accompanied by the release of an electron and vice versa.

$$Me \rightleftharpoons Me^{+} + e^{-} \qquad \text{(Eq. 1)}$$

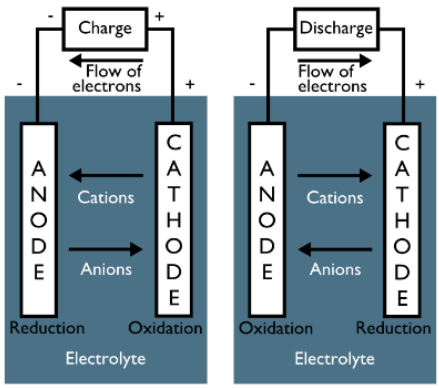

Figure 2: Diagram of a battery during charging and discharging [9]

The fundamental reaction behind batteries is called a redox reaction combining the oxidation and reduction half cell reactions. The anode is the sodium and electron source when discharging and is thus oxidized, shown in Equation 2. Simultaneously the cathode is reduced, shown in Equation 3. During this process the cathode consumes electrons released from the anode and intercalates an equal number of sodium ions from the electrolyte. During charging the process is reversed and the equations below would be flipped.

$$Na_xAnode(s) \rightleftharpoons yNa^+(aq) + ye^- + Na_{x-y}Anode(s) \quad \text{(Eq. 2)}$$
$$Na_zCathode(s) + yNa^+(aq) + ye^- \rightleftharpoons Na_{y+z}Cathode(s) \quad \text{(Eq. 3)}$$

The electrolyte is simply a medium for which sodium ions can be conducted back and forth between the anode and cathode. It additionally severs as a sodium ion reservoir. High conductivity is essential in the electrolyte in order to avoid it being a rate limiting factor in battery performance. Many factors can affect the ion mobility in the electrolyte including the type of solvent, electrolyte salt, molar ratio/concentration, and temperature. Furthermore, the electrolyte can greatly influence the operating voltage window of a cell. Outside of the stability window (see below) decomposition reactions require lower energy and will thus occur instead of the desired reactions.

2.2 Stability Window of Water

As previously mentioned using an aqueous electrolyte addresses many of the challenges currently faced with traditional electrolytes, primarily safety issues. Additionally, there are much cheaper alternatives, both in terms of raw materials (water and salt) and production. Aqueous electrolytes have been shown to have higher ionic conductivity than organic ones, which can oftentimes lead to higher (dis)charge rates. This makes them even more suitable to large scale grid stabilization [18]. In spite of this aqueous electrolytes have a limited stability window of 1.23 V. This is a somewhat significant hindrance compared to the 3-4 V of many standard organic electrolytes. To cope with the reduced stability window for aqueous cell operation the half cell potentials must be cut off at specific voltages in order to avoid the O_2 and/or H_2 evolutions.

The redox potentials for water are also pH dependent and can be plotted in a Pourbaix diagram. Normally they can be plotted against the standard hydrogen electrode (SHE), but knowing the potential difference between the Standard Hydrogen Electrode (SHE) and Na/Na^+ and the silver/silver chloride reference electrode we can easily adjust the axis to fit the potential range of a desired electrode. The derivation on the equations can be found in the Appendix. The alternate axes can be plotted knowing that the redox potentials of sodium are 2.71 V greater than that of the SHE and the redox potentials of Ag/AgCl are -0.21 V less than that of the SHE. The first point to notice is the rather significant difference between the theoretical and practical evolution lines. These overpotentials give a certain leniency with the stability window, but must be determined experimentally.

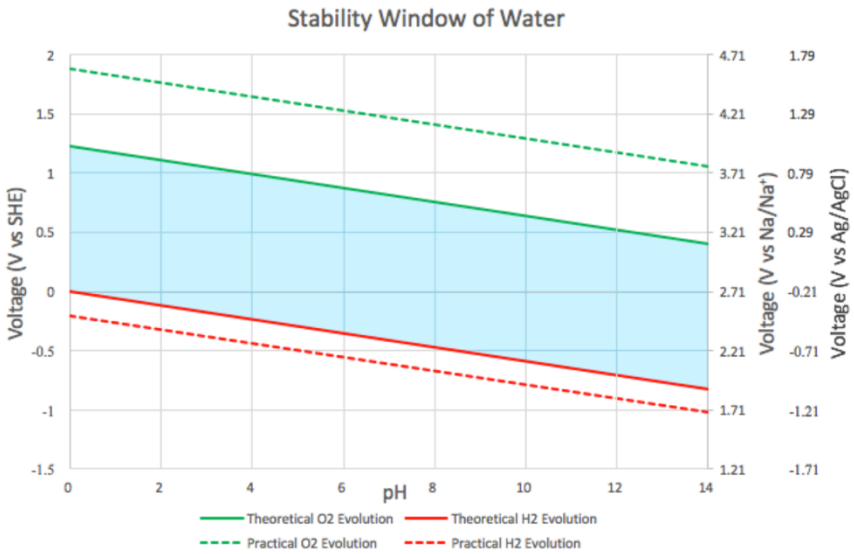

Figure 3: Pourbaix Diagram for H_2O

The Pourbaix diagram is be essential for determining the feasibility of electrodes, determining their cutoff potentials, and selecting the pH of the electrolyte. Using the reference electrode will also allow us to see which electrode might be having problems. For example, given the smaller overpotential for H_2 it might be more likely to have problems with the anode.

2.3 Criteria for Electrode Selection

There is a wide variety of materials available and one could spend an extraordinarily large amount of time just parsing through all the relevant literature. In an effort to simplify the selection process some additional constraints were added. These criteria also served to ensure that the selection process stayed in line with the overall goal of creating cheap large scale storage.

Naturally the first criterion was related to the materials electrochemical performance. Since there are many ways to evaluate the performance of a given material, it was vital to find the attributes most relevant for this project. Instead of high capacities and impressive charging rates it was more important to select materials that had a highly stable performance for extended lifespans (several hundred cycles). These materials should display good reversibility and therefore have minimal capacity fading over time. While materials with high capacities were preferred, those with lowers capacities but longer lives would be prioritized.

The materials used should also contain abundant elements and avoid rare metals. The reason was two fold, abundant elements hence the name are abundant and also much cheaper than conventional battery materials. For large scale production this could reduce geographic constraints and costs. For these reasons organic materials were ideal as they use primarily oxygen, carbon, and hydrogen, which are some of the most abundant elements. It would also be ideal to further constrain the search by limiting among abundant elements those that would be removed from their natural cycle, such as phosphorus and nitrogen [19][49]. One step further would be to ensure that the materials are chosen could be easily broken down and recycled/re-used. However, these constraints would begin to overcomplicate things, so they were omitted.

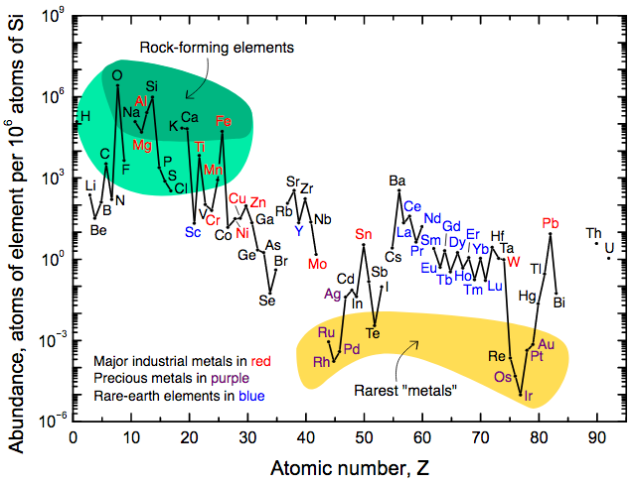

Figure 4: Elemental Abundance in the Earth's Crust [15]

The last constraint had to do with the ease of production. The materials themselves should not be too difficult to work with (eg. toxic/hazardous) or require complicated setups or processing steps. Energy intensive synthesis (eg. high temperatures) should also be avoided. Therefore even ideal materials would be disqualified if their syntheses involves many steps, requires too many ingredients, or is overly complicated. Doing so would facilitate straightforward and easy syntheses that are cheap and scalable.

3 Material Selection

The material selection chapter is incredibly vital because it justifies the material choices and explains why they were considered for this project. Even if the experiments were as well designed as could possibly be, if the materials used are selected without proper logical thought, then no matter the quality of the experimental setup the output might as well be useless. The materials chosen set up the foundation for the experimental work to come and should support the goals of the project. In this case selecting materials becomes a matter of choosing electrodes, such that some are already known to be stable with sodium (aqueous), while others are only proposed to be workable through preliminary experiments or density functional theory (DFT). Thus the resulting combinations could potentially yield a new electrochemistry based on existing materials that are proven, but not in a full aqueous cell. Other material choices, such as current collectors and electrolytes are made to support the electrode choices and facilitate material testing in both organic and aqueous cells.

3.1 Cathodes

The cathodes selected for testing had all the same criteria as mentioned in section 2.3, however it was necessary to add two additional criteria. The first was that the materials already contained sodium, since the anodes selected would not not contain sodium at the beginning and their operating potential needs to be in the upper region of the stability window. The second was that the materials have already been proven in literature because the primary goal was to research anodes. Therefore, using proven cathodes would limit complexity and allow for greater focus on the research materials: anodes.

3.1.1 $Na_{0.44}MnO_2$

For a longtime the general Na_xMnO_2 form of sodium manganese oxide with $x<1$ has been known to be suitable material for cathodes. The orthorhombic structure has performed very well in half cells against sodium and has a maximum theoretical capacity of 163 mAh/g. However, this number is highly dependent on the x value in Na_x per manganese oxide. The minimum and maximum values for x are 0.2 and 0.75 respectively. The upper limit is decided by the fact that for values larger than $x=0.75$ it become increasingly difficult to pass a current and the material subsequently suffers from degradation [7]. Therefore, the actual the theoretical capacity of any given Na_xMnO_2 material is determined by the x value.

The $Na_{0.44}MnO_2$ variety of sodium manganese oxide has been widely used due to its stability and performance in extended cycling. One study has even found the material to show little degradation after >2000 cycles with little to no capacity loss [47]. Conversely, starting with with a lower sodium content reduces the theoretical capacity to 66 mAh/g. Even though the sodium content could be higher it reduces stability and for $0.7 \leq x \leq 1$ the material behaves as an excellent super capacitor, yet this is not our goal [33]. Also, of all the possible phases, $Na_{0.44}MnO_2$ has been used far more frequently than the others, thus there is already sufficient evidence of its ability to function as a cathode against sodium. For these reasons it was chosen as one of the cathodes.

3.1.2 $Na_{0.65}MnO_2$

Considering the variety of sodium manganese oxides, naturally it seemed logical to try another more sodium rich Na phase as well. Tevar and Whitacre who have worked extensively with $Na_{0.44}MnO_2$ had also done a very nice study experimenting with many variations from $x=0.33$ to $x=0.7$. Some of their results are shown below [40].

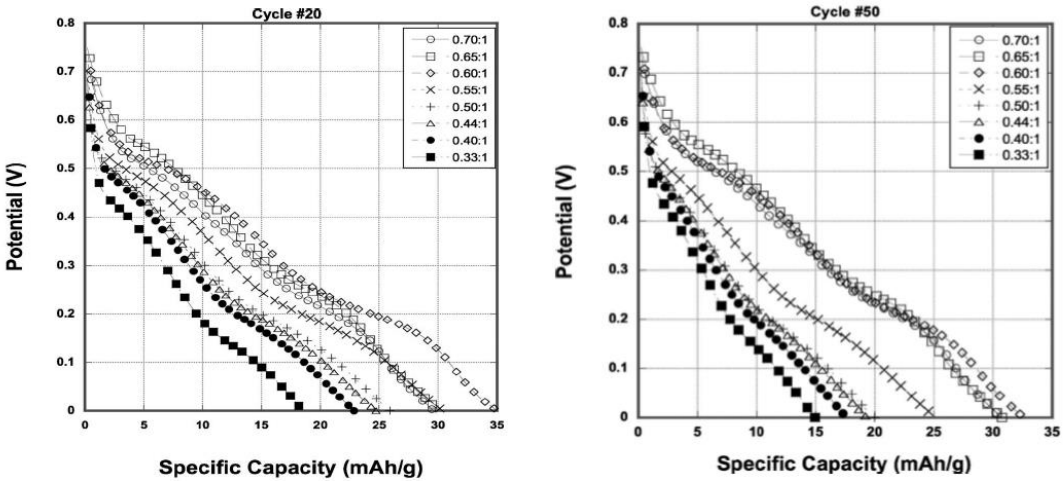

Figure 5: Potential vs Specific Capacity for All Na:MnO_2 Ratios After 20 and 50 Cycles [40]

Based on the graphs it seemed that higher sodium content leads to increased capacity, which is a natural conclusion. More importantly though, their capacities degraded at different rates. This was a valuable attribute to keep in mind when selecting a material as longer lifecycle with a stable capacity was more desirable than a high initial cycling capacity. These differences were more apparent in the following graph. $Na_{0.6}MnO_2$ started well, but appeared to degrade faster than the other high Na:MnO_2 ratios. The 0.65 and 0.7 ratios ended up having nearly identical performances and displayed reasonable capacities that seemed to increase and stabilize rather than deteriorate in time. Since the 0.7 ration is close the the limit at which it becomes unfeasible to intercalate sodium and the behavior becomes more capacitive, the 0.65 ratio was chosen. $Na_{0.65}MnO_2$ will offer the same specific capacity as the 0.7 ratio, yet with reduced risk of reaching the materials compete sodiation point and thus have better sodium intercalation.

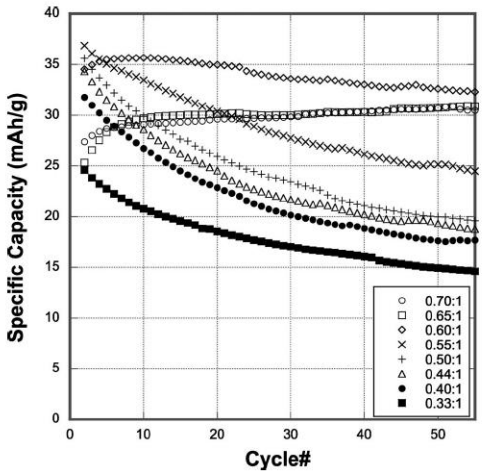

Figure 6: Specific Capacity vs Cycle for All Na:MnO_2 Ratios [40]

3.1.3 λ-MnO_2

The first thing to note about λ-MnO_2 is that it actually does not meet the first of the additional criteria, which required cathodes to already contain sodium. However, the spinel phase of MnO_2 is widely known to be an excellent host material for various ions, including sodium. In a study by Whitacre λ-MnO_2 is shown to have more than twice as much capacity as $Na_{0.44}MnO_2$ per kilogram. In addition, it has already been shown that the specific cost in $/kWh, which is

estimated to be <100 $/kWh, is already significantly less than that of other materials and it is completely stable in aqueous electrolytes [47].

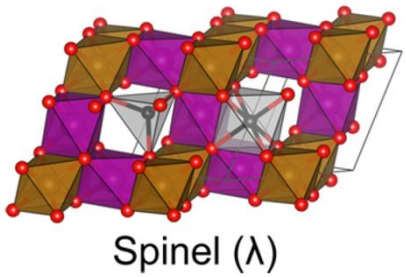

Figure 7: λ-MnO_2 – The purple and yellow spheres represent Mn atoms are inside MnO_6 octahedra while the black spheres in grey octahedra represent potential intercalation sites [21]

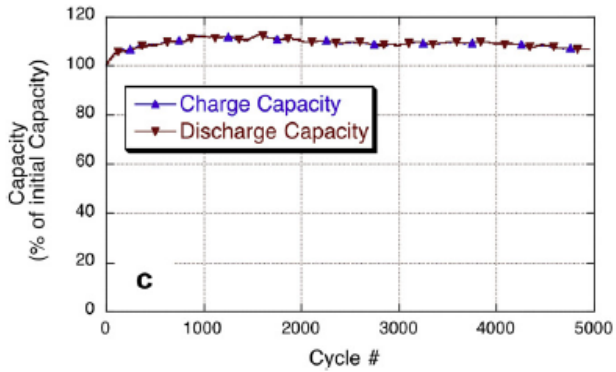

Figure 8: λ-MnO_2 Long Term Cycling [47]

Furthermore the materials high specific capacity has been proven to be around 100 mAh/g and experiments have shown that it can be cycled at high C rates and maintain this capacity for up to 5000 cycles while maintaining its initial capacity of 100 mAh/g [47][55]. All these factors combined make the spinel phase a very worthwhile cathode to use. The fact that it does not initially contain sodium can also be dealt with by cycling it against a sodium containing material. After a couple cycles when sodium is inserted into the structure the cell can be taken apart, the sodiated spinel cathode removed, then inserted into a new cell to be cycled against a particular anode.

3.2 Anodes

The anodes considered in this project were also subject to the same criteria mentioned in section 2.3. Since anodes were the intended research material it was vital to pick compounds that had some apparent potential, yet were not completely proven in full and/or aqueous cells. In the past anthraquinone has been researched at the Reactor Institute of Delft as a negative electrode for sodium aqueous batteries. Due to the prior experience and optimistic research with this material, other organic compounds were considered and ultimately the naphthalene group of materials was further investigated. Because of past solubility issues the organic compounds were chosen with an additional criterion being that they could be made into polymers.

3.2.1 Polyanthraquinone

Anthraquinone by itself has been a used as an anode for lithium batteries. Opposed to the typical intercalation process of crystalline materials, when cycled against lithium it at has a capacity of 200 mAh/g and given the comparable sizes of lithium and sodium ions it would be

feasible to bond with sodium [53]. In one study where it was cycled against sodium capacities of 100 mAh/g were realized, while even higher capacities of 200 mAh/g were obtained with higher salt concentration in the electrolyte [13]. Furthermore, the compound is completely organic, which is ideal for finding electrodes made of abundant elements and it has quite a long and flat voltage plateau upon (dis)charge. Another advantage is that the material in insoluble in water, which is a rather desirable quality since it is intended to be used with an aqueous electrolyte [17]. However, being organic this means that opposed to the typical intercalation process of crystalline materials, anthraquinone bonds to sodium in a two step reaction with the oxygen atoms as shown in Figure 10.

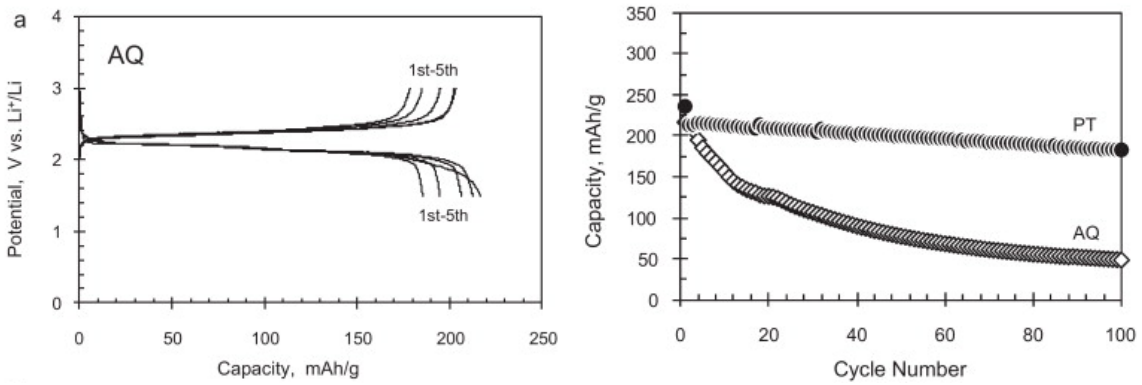

Figure 9: a. (Dis)Charge curves of Anthraquinone b. Capacity vs Cycle of AQ [17]

A point of interest is the rapid capacity fading of anthraquinone. In its initial cycles it achieves a quite high capacity of 225 mAh/g which is 88% of its theoretical capacity of 257 mAh/g. However, the performance rapidly declines and this has widely been attributed to anthraquinone dissolution into the electrolyte. While anthraquinone is supposed to be insoluble in water it has been known to dissolve into organic electrolytes [44]. In previous research within our group it has also been found that once anthraquinone bonds with sodium it then becomes semi-soluble in even aqueous electrolytes leading to electrode dissolution and rapid capacity fading. Conversely, this behavior is not reported in literature versus Na^+ in organic electrolyte [13].

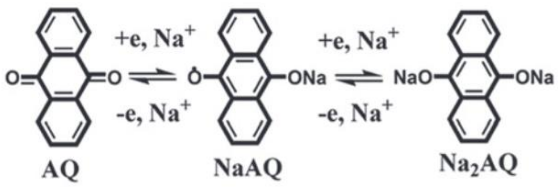

Figure 10: Bonding scheme of Anthraquinone with Na^+ (AQ) [13]

In an effort to mitigate these effects while retaining the electrochemical performance of the material one idea was to make it into organic polymer, polyanthraquinone. Polymers are large chains of repeating sub-units known as the monomer, which are attached together with a linking molecule. Making a linked structure would reduce the solubility and increase structural integrity while maintaining the same electrochemical performance. Therefore, polyanthraquinone was chosen as one of the research materials.

3.2.2 PNTCDA

Another interesting organic monomer was NTCDA, formally known as 1,4,5,8-naphthalenetetracarboxylic dianhydride. The material has shown promise both in DFT and in

experimental work. The material can also be made into a polymer, which would be valuable in avoiding solubility issues as well as making it more robust. The name of said polymer is polyimide 1,4,5,8-naphthalenetetracarboxylic dianhydride or PNTCDA [29].

The NTCDA monomers can be joined together with several different linkers and have the possibility of adding functional groups to tailor the compound to either make it more electron withdrawing or donating [1]. More importantly though the basic NTCDA structure can bond up to 4 sodium ions giving it a rather high theoretical capacity of 279 mAh/g. Unfortunately, realizing this high capacity has been a challenge in all literature reviewed during this project and the practical capacity is much less [45]. However, the bonding mechanism of PNTCDA has been observed to be a two phase reaction by DFT as shown below.

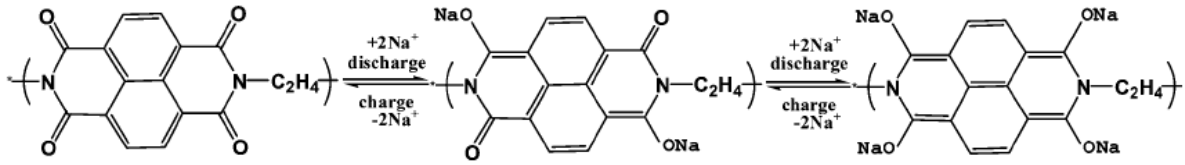

Figure 11: Two step reaction of PNTCDA with C_2H_4 linker [45]

Based on the charge (dis)charge curves of PNTCDA and its long term cycling performance the practical capacity is 140 mAh/g. Therefore it suggests that only the first step of the reaction is occurring. In fact, recalculating the theoretical capacity under the assumption that only two sodium ions bond yields a theoretical capacity of 140 mAh/g which aligns exactly with the experimental work. Furthermore, the (dis)charge curves only have one long plateau seemingly corresponding to the bonding of the first two sodium ions. Two plateaus would normally be expected for such a two step reaction. This further indicates that the full capacity cannot be obtained. In literature, some have tried discharging the material to voltages lower than 1.2 V, but they report this being accompanied by severe structural damage inhibiting functionality. Therefore, it appears that the full theoretical capacity of 4 bonded sodium ions is currently unattainable. Nevertheless, it works very well with the first sodium ion pair [3].

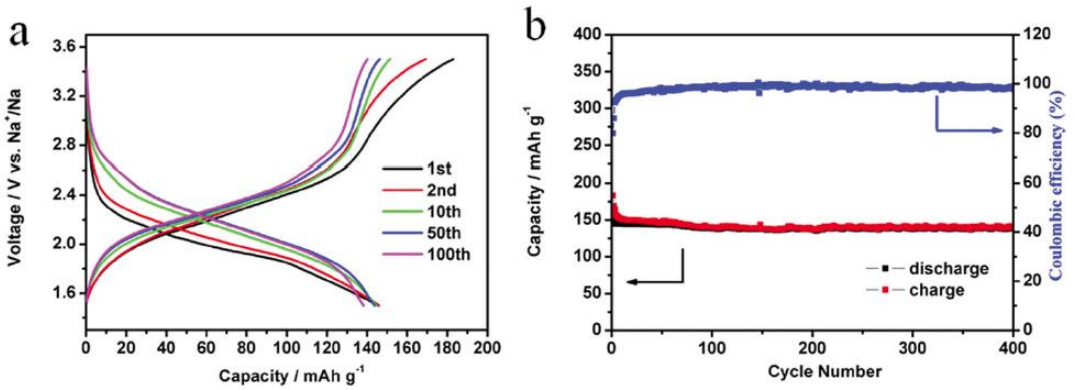

Figure 12: (a) (Dis)Charge Curves of PNTCDA (b) Capacity vs Cycle of PNTCDA [45]

Another point worth noting from the (dis)charge curves is that they go to 1.5 V which is outside the stability window of water, yet the entirety of the voltage plateau is above 2 V which is workable within the stability window. Therefore, in aqueous testing the limited voltage range should not interfere with the material bonding with sodium. Also the material has been proven stable to 5000 cycles at a 0.8C rate and can even be cycled at C-rates as high as 30C designating it suitable for high power applications. Lastly, the synthesis is rather straightforward and uses only very common materials [3][45].

3.2.3 Naphthalimide

Naphthalimide is perhaps the most interesting choice of material because it is not yet proven as an electrode. This one in particular is a variant form of the naphthalimide shown in Figure 13. While there are a couple researchers who have written about its use in lithium batteries, at the time of writing there is no known literature speaking of its use in full cells, let alone for sodium batteries [25]. However, the naphthalene diimide and perylene diimide families of compounds has been well documented performing well with lithium and sodium when in polymer form. In fact, these groups have been made into covalent organic frameworks known as COFs which have started to be seriously investigated as battery anodes [51].

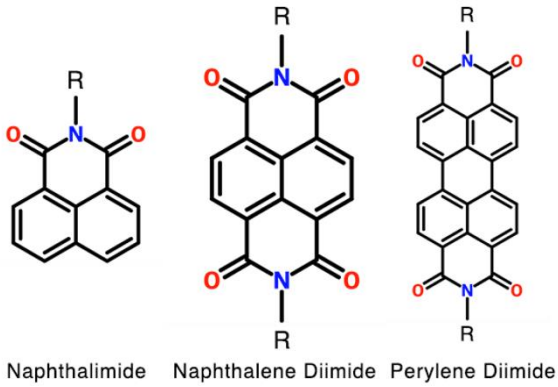

Figure 13: Three compound families

Since naphthalimide is very these similar to these other compounds it seemed highly possible that it could work as an anode. Additionally, it would be the first time it was used in a sodium battery and could possibly lead to higher specific capacities compared to the other materials investigated in this project. This is due to the fact that naphthalimide could potentially bond with two sodium ions and has a lower molecular weight compared to the other compounds. Also it meets the requirements for materials selection as it only needs the additional of a hexanol tail to the basic naphthalimide in order to functionalize it for polymerization and this process is a short and simple one step low temperature synthesis.

An additional point about these materials in general is that the benzene rings and linkers for their polymerized forms play important roles in the material performance. The additional benzene rings tend to improve the material's thermal and cycling stability in addition to reducing the solubility. The smaller the linker the higher the specific capacity (eg. $(CH_2)_2$ instead of $(CH_2)_4$ connecting the monomers, R in in Figure 13) [2][45].

3.3 Electrolytes

Naturally, since the nature of this project was to make aqueous batteries an aqueous electrolyte was used. However, before even getting that far many tests would be needed to be conducted against sodium metal in half cells. These experiments would require a stable and reputable organic electrolyte. Only after confirming the performance of materials and feasibility of certain chemistries could we move forward to full cell aqueous testing.

3.3.1 Organic

The organic electrolyte chosen is 1M sodium perchlorate ($NaClO_4$) in ethylene carbonate (EC) and dimethyl carbonate (DMC) mixed in a 1:1 volumetric ratio. Most organic electrolytes used

for sodium ion batteries use the EC/DMC combination with a various sodium salts. The EC/DMC combination has been shown to have a high conductivity and induce passivation on the current collectors. Therefore, the EC/DMC electrolyte is well documented and sodium perchlorate as the salt has been known to function well for sodium ion batteries. For these reasons it was chosen to be used for testing [14].

3.3.2 Aqueous

There are several possible salts and many pH levels that could be used for an aqueous electrolyte. One combination that was very prevalent in literature was 0.5M sodium sulfate (Na_2SO_4) at pH 7. As pH 7 is neutral it is very safe and most likely inert with our electrode materials. It is likely that the material potentials will be within the pH 7 stability window and if this is not the case it can be adjusted accordingly later on. Once reduced the SO_4^{2-} anions can react with the H^+ or other SO_4^{2-} ions in the aqueous electrolyte, however these redox potentials are outside the stability window of water (they occur at -1.925 V and -1.175 V vs Ag/AgCl in pH 7 respectively). This is ideal as it means that during operation within the stability window of water the only redox reaction in the electrolyte will be uniquely with sodium [20].

An important note about the aqueous electrolyte is that it must be completely purged of O_2 before testing. Any oxygen within the water will bond to the sodium, which depletes the capacity and can lead to other unwanted side reactions, which in turn leads to an undesirable performance.

3.4 Current Collectors

The last part of the cell to be selected is the current collectors. These need to be inert and stable within the working potential range of the cell during testing. If not, they can become unstable and disturb the performance of the materials because of unfavorable side reactions. Therefore, efforts were made to match the current collectors used in literature.

3.4.1 Organic

In organic electrolyte aluminum foil was used as the collector material for both anodes and cathodes. Almost all literature reviewed indicated that aluminum was stable with the anode materials, so naturally this was used [3][17]. The cathode materials have been made into electrodes either using coatings with polyvinylidene fluoride (PVDF) and carbon black or making pellets with polytetrafluoroethylene (PTFE) and carbon black [24][48]. Both methods yielded electrodes delivering the same performance and since coatings were easier to make aluminum was selected.

3.4.2 Aqueous

Most recently carbon cloth had been used as the current collector for aqueous testing within the group. It has been used in literature and since we have used it before it is readily available and familiar [31]. During the initial testing of the aqueous setup electrodes were also made with stainless steel grid mesh. These gave similar results, but were quite difficult and inconvenient to work with. Therefore, carbon cloth remained the current collector of choice.

4 Experimental

In the following sections the details of the material synthesis, electrolyte preparation, and electrode fabrication are described. The cathode materials, which can be easily made by solid-state synthesis and acid leaching are characterized by X-ray diffraction (XRD) while the organic polymers for the anodes are characterized by liquid nuclear magnetic resonance (NMR).

4.1 Cathodes

4.1.1 $Na_{0.44}MnO_2$

Sodium carbonate (J.T. Baker) and manganese (III) oxide (Sigma Aldrich) were used as the precursor materials for sodium manganese oxide. The reaction is as follows.

$$8(Na_2CO_3) + 18(Mn_2O_3) + 5O_2 \rightarrow 4(Na_4Mn_9O_{18}) + 8(CO_2) \quad \text{(Eq. 4)}$$

In reality some of the sodium is lost either in preparation or it is not fully reacted during synthesis, so it is necessary to add some excess sodium carbonate in order to achieve the desired ratio. Fortunately, since $Na_{0.44}MnO_2$ is well documented it is known that a 0.55:1 ratio is necessary to achieve a synthesized 0.44:1 ratio. This corresponded to 1.467 g (155.5 mmol) of Na_2CO_3 and 3.95 g (623 mmol) of Mn_2O_3 which were then mixed together and ball milled at slow speed for 2 hours. Afterwards the material was placed in a crucible and heated at 800° C for 12 hours. The ramping rate was roughly 5° C/minute [48].

The material was then characterized by XRD and the spectrum is shown below. The spectrum contains more peaks than shown in literature, yet aligns much better with the peak list provided by the Joint Committee on Powder Diffraction Standards (JCPDS), which is shown in the Appendix. For example, the peaks up to the 20° 2θ angle are in fact doublets and other minor peaks at higher angles are indeed supposed to be present.

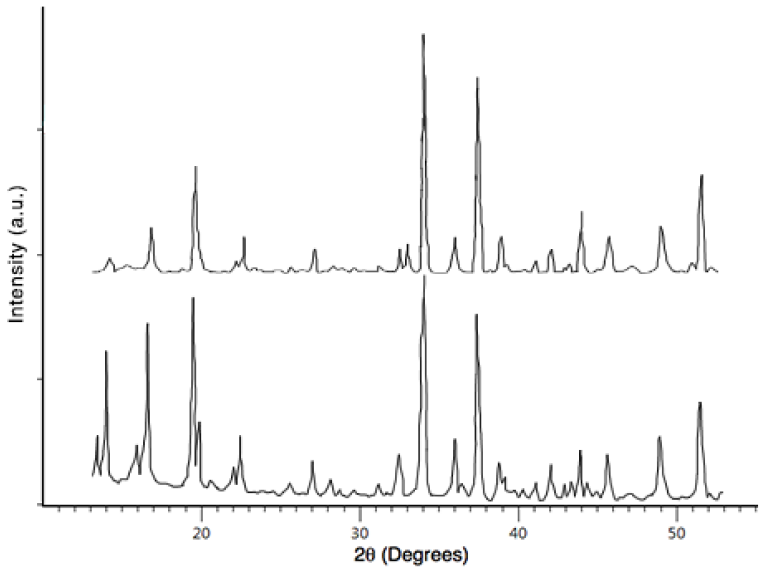

Figure 14: XRD Spectrum of $Na_{0.44}MnO2$ compared to literature (top) [48]

4.1.2 $Na_{0.66}MnO_2$

The 0.65 version of sodium manganese oxide is synthesized in exactly the same method as described above, but naturally the starting precursor ratios are different. The ideal reaction is as follows.

$$130(Na_2CO_3) + 200(Mn_2O_3) + 35O_2 \rightarrow 4(Na_{65}Mn_{100}O_{200}) + 130(CO_2) \qquad \text{(Eq. 5)}$$

However, as was the case before an excess of sodium carbonate is necessary. The proper precursor ratio was found to be 0.73:1 in order to yield 0.66:1 which is not 0.65 exactly, yet was sufficiently close. This corresponded to 1.934 g (205 mmol) of Na_2CO_3 and 3.95 g (623 mmol) of Mn_2O_3. Since the synthesized material was $Na_{0.66}MnO_2$ it is referred to as such throughout the report even though the desired material was $Na_{0.65}MnO_2$.

In the study where multiple phases were synthesized a relationship was drawn relating the precursor ratio and synthesized ratio. While the relationship was linear, the proportions were arbitrary as to which phases required 10% excess of sodium versus 30% [40]. Therefore, when the synthesis was first attempted using the precursor ratio from literature the sodium content was much lower than the intended $Na_{0.65}$/Mn. Based on this first result the $Na_{0.73}$:Mn precursor ratio was found. The extra sodium carbonate content is most likely required as during the heating process excess O_2 CO_2 are formed leaving Na_2O.

The material was then characterized by XRD and the spectrum is shown below. At the time of writing, there was only one article showing the spectrum for $Na_{0.65}MnO_2$ and it only covers 15° of early two theta angles [40]. This meant that any comparison would only show the first tall peak, which is rather insignificant for comparing to the entire spectrum given by XRD. To be certain of the material an analysis was made using the JCPDS data as reference, which is shown in the Appendix.

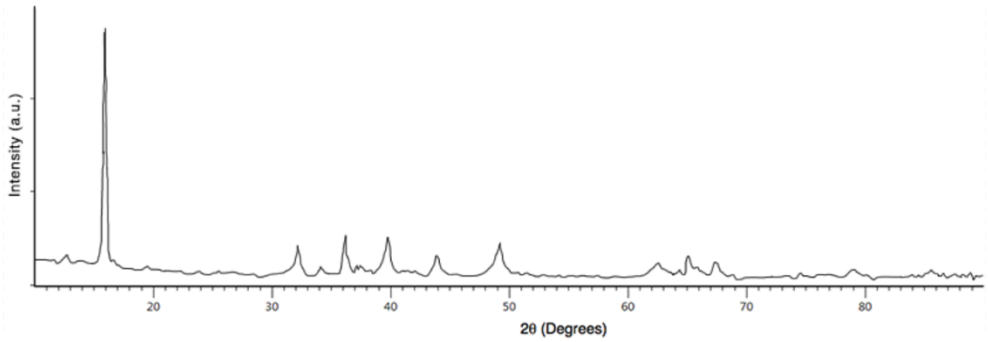

Figure 15: XRD Spectrum of $Na_{0.66}MnO2$

4.1.3 λ-MnO_2

The spinel phase of MnO_2 can be obtained by chemical leaching. The λ-MnO_2 was prepared by loading 5 g (884 mmmol) of $LiMn_2O_4$ (Sigma Aldrich) into a beaker and then adding 200 mL of distilled water. Next 10 mL of HCl (Alfa Aesar 36.5 – 38%) was added slowly. The mixture was left stirring over night. The following day the stirring was switch off and the material was allowed to settle. Once the material accumulated at the bottom of the beaker, as much water as possible was pipetted out while avoiding material loss. Then the material in the beaker was washed with ethanol and distilled water multiple times. Once everything evaporated the dry powder material was collected [6].

Other acids could be used and filtration would be a much faster collection method [16].

The material was then characterized by XRD and the spectrum is shown below. It is nearly a perfect match with literature and the JCPDS data shown in the Appendix.

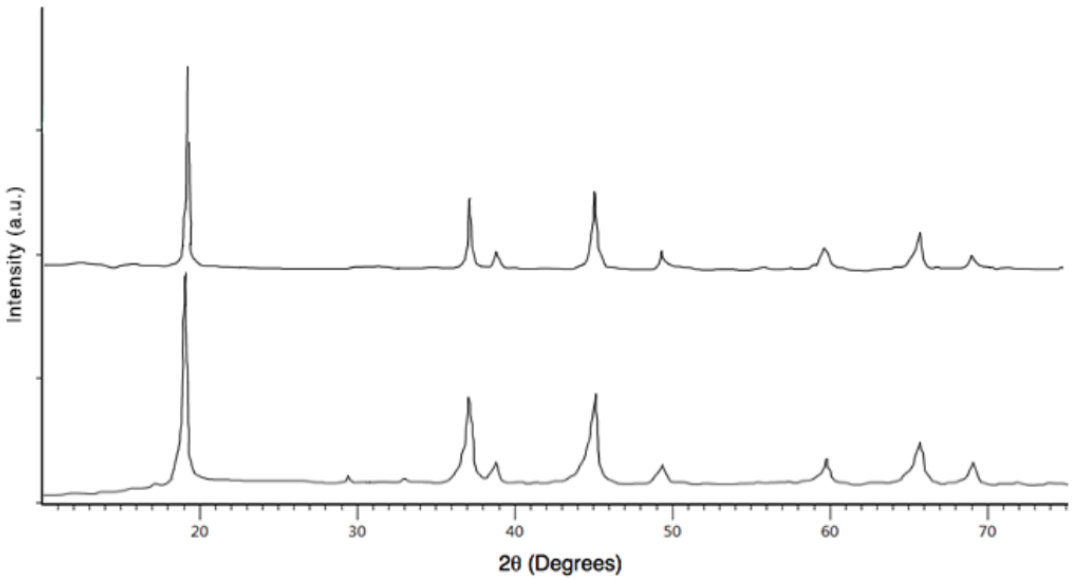

Figure 16: XRD Spectrum of λ-MnO2 compared to literature (top) [55]

4.2 Anodes

4.2.1 Polyanthaquinone

The synthesis of polyanthraquinone, also formally known as hydroxyhexyloxyanthraquinone, is started with 2-hydroxyanthraquinone (1.54 g, 6.9 mmol), 6-bromo-1-hexanol (1.25 g) (Sigma Aldrich), and K_2CO_3 (2.375 g) mixed together in a flask of 24 mL of dimethylformamide (DMF) (Sigma Aldrich). The mixture was stirred overnight under an argon atmosphere. The mixture was cooled to room temperature and then filtered. It is then washed with dichloromethane (VWR) and ethyl acetate (VWR). The product was then collected (1.6 g, 6.175 mmol, 89% yield) [34]. Below is a diagram of the synthesis and the NMR spectrum of the raw material can be found in the Appendix.

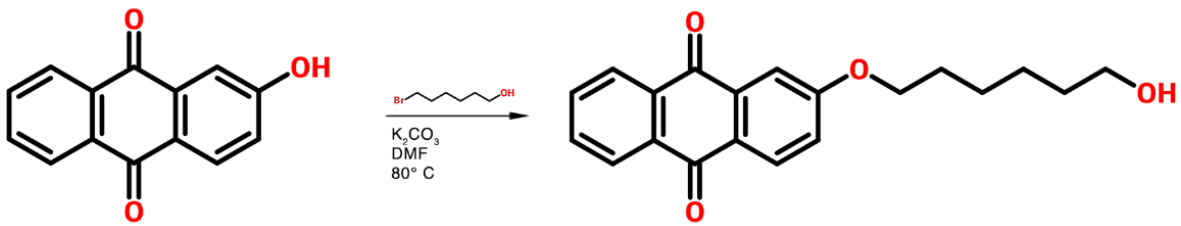

Figure 17: Synthesis of Polyanthraquinone

As the material still contained many impurities it was necessary to purify it by column chromatography. A column was stacked with silica gel and eluted with a solvent mixture of dichloromethane and ethyl acetate in a 4:1 ratio. The vials collected were compared to the raw product using thin layer chromatography. Then the vials containing the product were identified and mixed back together in a round bottom flask for rotary evaporation [34]. This yielded a yellow solid product (1.62 g, 5 mmol, 72% yield). The NMR spectrum for the final product

can be found in the Appendix. NMR analysis software (MestReNova) was then used to identify the H^+ with the corresponding peak/integration value.

4.2.2 PNTCDA

The synthesis for PNTCDA mostly followed the method described in an article by Sassi et al. [35]. However, after attempting their method as described several times it was not possible to properly synthesize the material at all or synthesize it with adequate level of purity. The following describes the method used, which is loosely adapted from their reaction. It is by no means ideal and could certainly be simplified.

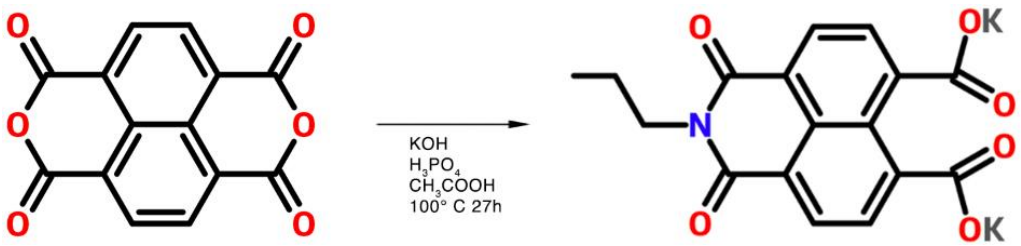

Figure 18: NTCDA Synthesis Step 1

To begin, 425 mL of distilled water is poured into a large flask. Then 2.5 g (9.32 mmol) of naphthalene dianhydride (Sigma Aldrich) is added. A 1M solution of potassium hydroxide corresponding to 2.302 g (41 mmol) of KOH (Alfa Aesar) dissolved into 41 mL of distilled water was added into the suspension. The mixture was heated to 60° C while stirring to obtain a clear amber solution. Next the mixture was acidified with 1M of phosphoric acid corresponding to 1.34 g (13.6 mmol) of H_3PO_4 (Sigma Aldrich) dissolved into 13.67 mL of distilled water. At this point the pH should be 6.5. Then the mixture was slightly neutralized by 0.55 g (9.32 mmol) of propylamine (Sigma Aldrich) followed by re-acidifying the solution to pH 6.3 with the another 1.34 g (13.6 mmol) of H_3PO_4 dissolved into 13.67 mL of distilled water. Then the solution was left stirring while heated to 100° C for 27 hours with reflux [35].

At this point, according to literature, it should be possible to obtain the monoanhydride. However, this was not the case, so the steps listed in the following paragraph were added.

After cooling back down to room temperature another 1M solution of potassium hydroxide was added, this time 2.805 g (50 mmol) of KOH in 50 mL of distilled water. Then phosphoric acid was added dropwise until a pH of 6.5 was obtained as measured with a pH meter. The solution was then left stirring while heated to 100° C for 27 hours with reflux again. After cooling to room temperature 12.5 mL of acetic acid was added dropwise to the solution. It was left stirring for 20 minutes while observing the formation of a precipitate. Afterwards the solid product was filtered off and left to dry at 60° C under vacuum (1.6 g, 4.89 mmol, 52% yield). The material was characterized by NMR and the spectrum is shown in the Appendix.

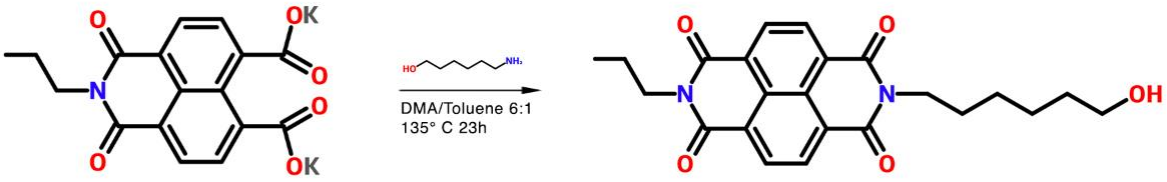

Figure 19: NTCDA Synthesis Step 2

In a closed schlenk flask under argon atmosphere a mixture of the of the product (1,4,5,8-naphthalenetetracarboxylic acid 1,8-monoanhydride) (800 mg, 2.4 mmol) and 6-amino hexanol (286 mg) (Sigma Aldrich) was made. A mixture of 8 mL of dimethylacetamide (DMA) (Sigma Aldrich) and 1.33 mL of toluene (VWR) was then added into the flask as well. The mixture was heated to 135° C for 23 hours and then allowed to cool to room temperature. The precipitate was collected by filtration and then dried in a vacuum oven (620 mg, 1.76 mmol, 72% yield) [35].

The resulting NTCDA was still not pure, so a recrystallization was necessary. The material was loaded into a round bottom flask and ethanol was used as the solvent. The mixture was then heated to about 85° C while under reflux. If after an hour material had still not dissolved more ethanol was added. Once all the material had dissolved the mixture was allowed to cool naturally and then filtered. The remaining product was characterized by NMR and the spectrum can be found in the Appendix. NMR analysis software (MestReNova) was then used to identify the H^+ with the corresponding peak/integration value.

4.2.3 Naphthalimide

The naphthalimide used in this research is formally known as N-6-hexanol-1,8-naphthalimide as the only difference between this and the base compound is the hexanol tail. The synthesis begins by loading 3.35 g (17 mmol) of 1,8-naphthalic anhydride into a flask with 250 mL of DMA. Then 4 g (34 mmol) of 1-amio-6-hexanol in 20 mL of DMA is added dropwise over a period of 30 minutes into the suspension. The mixture is then stirred while heated to 100° C for 6 hours. Afterwards the solvents are removed by rotary evaporation and then 100 mL of demi-water is added to the residue causing a white precipitate which is the napthelenimide [23]. Lastly it is filtered off and dried (4.47 g, 14.9 mmol, 87% yield).

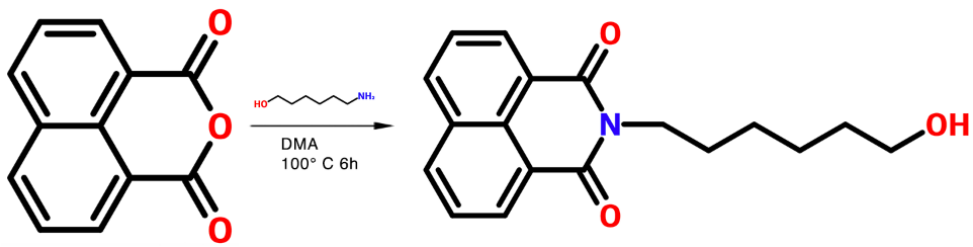

Figure 20: Naphthalimide Synthesis

The material was characterized by NMR and the spectrum can be found in the Appendix. NMR analysis software (MestReNova) was then used to identify the H^+ with the corresponding peak/integration value.

4.2.4 Polymerization

In order to simply to polymerization process all the final materials were polymerized by the same procedure. A general description is given and then the following table gives the precise quantities for the chemicals required to polymerize each compound.

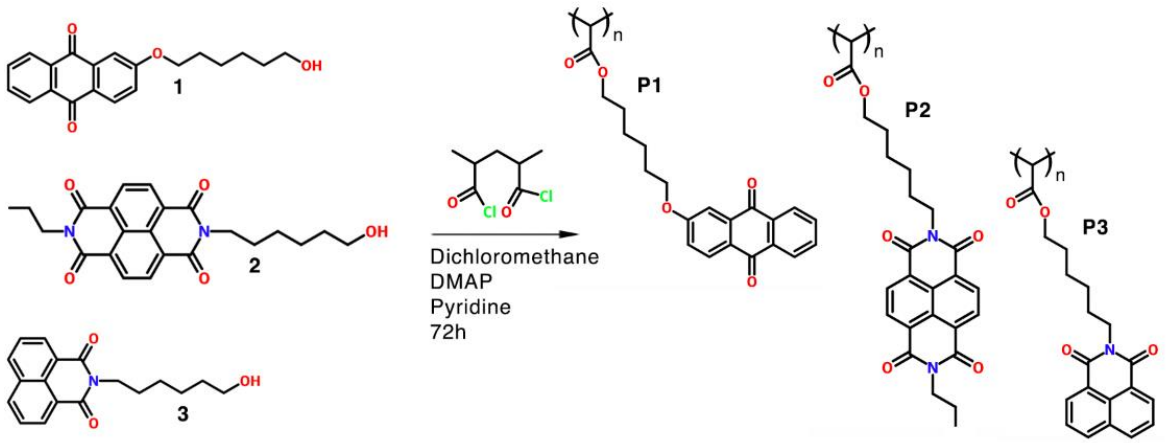

Figure 21: Polymerization

In a dried flask, pure compound was dissolved in dry dichloromethane and put under an argon atmosphere. Subsequently, 4-dimethylaminopyridine (DMAP), pyridine, and poly acryloyl chloride 25% in dioxane were added. The solution was mixed for 72 hours at room temperature. To quench the reactivity of the compound obtained, an excess of dry methanol was added. The mixture was stirred for 2 more hours at room temperature. Then the solution was precipitated in methanol and filtered. The polymer was purified by repeated precipitation from chloroform into methanol. The final pure polymer was then obtained.

Material	DCM	DMAP	Pyridine	Poly(a.c.)	MeOH	Polymer	Yield
Anthraquinone (**1**) – 1 g, 3.08 mmol	55 mL	16.7 mg 0.15 mmol	1.53 mL 19 mmol	1.08 mL 3.08 mmol	2.3 mL 56.4 mmol	Poly AQ. (**P1**)	N/A
NTCDA (**2**) – 0.5 g, 1.22 mmol	22.6 mL	7.5 mg 0.061 mmol	0.61 mL 7.55 mmol	0.43 mL 1.22 mmol	0.9 mL 15.3 mmol	PTNCDA (**P2**)	N/A
Naphthalimide (**3**) – 1.5 g, 5.04 mmol	80 mL	31 mg 0.25 mmol	2.5 mL 31.2 mmol	1.8 mL 5 mmol	3.7 mL 91.8 mmol	Naph. (**P3**) – 90 mg, 0.25 mmol	5%

Table 1: Measurements for Polymerization

4.3 Electrolytes

4.3.1 Organic

The organic electrolyte was made in a glove box. A 1M solution of $NaClO_4$ (Sigma Aldrich) is made in a 1:1 mixture of EC (Sigma Aldrich) and DMC (Sigma Aldrich) (ratio is calculated by volume). A volume of 25 mL of electrolyte can be made by dissolving 3.06 g (24.9 mmol) of sodium perchlorate in 16.52 g (18.7 mmol) of EC and 13.37 g (14.8 mmol) of DMC [22].

4.3.2 Aqueous

Since the aqueous cells used up 10 mL of electrolyte per cell, which is far more electrolyte than the organic cells, large batches of aqueous electrolyte were typically made. Normally, 35.51 g (250 mmol) of Na_2SO_4 (Sigma Aldrich 0.25 M) was dissolved into 0.5 L of distilled water to make pH 7 0.5M Na_2SO_4 aqueous electrolyte. It is worth noting that although it is technically a 0.5M ratio, since each sodium sulfate contains 2 sodium atoms it is a 1M ratio for sodium ions with respect to water. The last, but arguably most important step is to purge the oxygen that may already be in the water before use in the aqueous cell. To do so, the electrolyte is placed in an airtight container with two pressure valves. Through one valve nitrogen is pumped in while the electrolyte is stirred and through the other excess N_2 and O_2 can exit to relieve the pressure inside and purge the oxygen. After about 3 hours of purging the electrolyte is ready for use [3].

4.4 Coatings

All final materials were made into coatings to be used in the cells. These coating were made by mixing 80% active material, 10% carbon black (Timcal 45), and 10% PVDF (SOLEF 21216) by weight together. The 80/10/10 ratio is a standard for making coatings and maximizes active material while ensuring there is sufficient conductivity thanks to the carbon black and PVDF acts as a binder to hold everything together. The powder mix was then hand ground with a mortar and pestle to reduce the size of large agglomerated particles and further mix the materials. Then an appropriate amount of N-methyl-2-pyrrolidone (NMP) (Sigma Aldrich) was added to make the powder into a slurry. The amount depended on the active material and carbon black and was determined by experimentation. Once the slurry had the desired viscosity it was coated onto either aluminum or carbon cloth. The aluminum would be cleaned with acetone beforehand. A doctor blade was used to coat the slurry across the selected current collector and give the coating the required thickness. Afterwards the coated foil or cloth was placed in an oven and dried at 70° C for an hour at ambient pressure or left to air dry under a ventilation hood. It seemed the air drying gave more consistent results with fewer cracks even though it took longer, so this method was almost always used.

All half cell organic electrolyte positive electrodes used coatings of 200 μm thickness on aluminum foil while negative electrodes used coatings of 100 μm. All full cell aqueous electrolyte tests used coatings of 100 μm thickness on carbon cloth. The reason for same thickness coatings on carbon cloth negative and positive electrodes is because the material is a woven fabric, so additional material would be absorbed into the cloth making it difficult to achieve the desired mass loading.

4.5 Organic Cells

For organic half and full cell testing custom designed swagelock clamp cells were used. All assembly was done in an argon atmosphere glove box as to maintain an oxygen and moisture free environment. This was essential to keep materials pure and particularly for avoiding oxidation of the pure sodium disks that was often used as a counter electrode. Normally the anode was placed down first and then a glass fiber separator (Whatmann GF/C) was placed on top. Then several drops of electrolyte were pipetted onto the separator before placing the electrode on top and finally closing the cell.

4.6 Aqueous Cells

While there was an existing setup for testing aqueous cells, it was clunky and impractical. Fortunately, before this project was started a new custom cell had been designed and manufactured, which greatly improved and eased the cell assembly and testing process. The main advantages of the new design were that it required less electrolyte, had the electrodes closer together and added pressure for better contact, and was orders of magnitude faster to assemble/clean/etc. than the previous setup. A schematic of the cell is shown below.

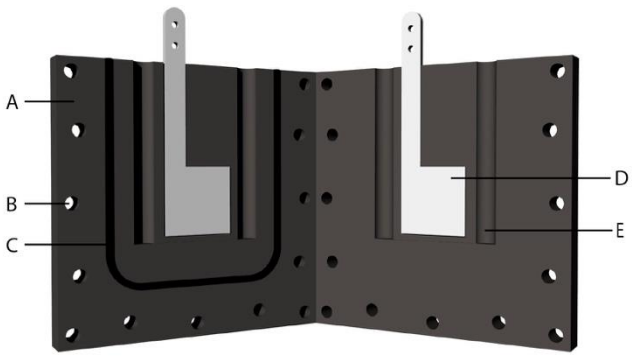

Figure 22: Cell Design – A. Cell body B. Screw holes C. Rubber gasket D. Stainless steel electrode plates E. Spacing for reference electrode(s)

The first important detail about the aqueous setup is the use of a reference electrode. As the setup was only used to test full cells, it was very valuable to have a reference electrode which could measure the individual half cell potentials. This would give a more detailed plot of the electrodes' performance and allow us to see O_2 and H_2 evolution independently. In line with previous research a double junction silver chloride (AgCl) electrode (Sigma Aldrich) was used. In a standard solution of 3M potassium chloride (KCl) the redox potential is 0.21 versus the SHE. The electrode was routinely tested for accuracy against a piece of copper foil, for which the standard measured potential should be 0.127 V versus Ag/AgCl under standard test conditions. During experimental work the potential was usually within 3% of the standard 0.127 V, which was suitable for testing.

In order to assemble a cell for aqueous testing the punched electrodes were placed on the stainless steel plates (D in Figure 22) with three separators between them. The reason for three separators is simple. With two separators the electrodes have too much room and slide around while with three they stay in place with sufficient pressure ensuring good contact between the electrodes. Four separators would provide even better pressure, but was not necessary. The cell could then be screwed together.

Before testing the cell was filled with aqueous electrolyte through one of the reference electrode holes before the reference electrode was rinsed with demi-water and placed inside. A key point is that the reference electrode was wrapped with several layers of Parafilm near the top to ensure an airtight closure. Since a second reference electrode was never used the second hole was blocked with conical wood block also wrapped in Parafilm.

5 Results and Discussion

This chapter covers the results of the synthesis and cell testing. The results of each experiment are presented followed by a brief analysis of what worked and what did not. Then some explanations are put forth as to what might have caused the issues encountered.

5.1 Synthesis Outcome

The major novelty to this project was the finding, synthesis, and testing of new anodes. As such, many problems and some of the most troublesome ones arose during the synthesis of these materials. It consisted of two steps, functionalizing the base compounds and then polymerizing them. While it was possible to create some of the materials, dealing with the hindrances of the synthesis proved to be a significant obstacle. In the end, the monomers had to be used as the test materials and the amount of time allotted for testing was relatively small. Understanding these difficulties can help in reducing synthesis time and increasing the overall synthesis yield.

5.1.1 NTCDA

NTCDA was by far the hardest material to make due to the fact that it required the addition of two different functional groups. Polymers can be made in a variety of ways and in almost all literature to date PNTCDA had been made as a linear polymer with NTCDA monomer units linked with an ethyl group end to end. This can only be done for monomers that have two points of attachment, unlike anthraquinone and naphthalimide. To perform non-linear polymerization of these compounds would require the addition of single functional group, which was 6-amino hexanol. This would facilitate a branched type of polymer with a poly acryloyl chloride backbone (see Figure 23). In order to have a simplified batch polymerization process it was decided to make NTCDA into the same type of branch polymer opposed to a linear one. However, this complicated things for NTCDA because it then required two different functionalizations. One side would be reacted with propylamine and the other with 6-amino hexanol. The first step which is to attach the propylamine to only one side of a symmetric compound (naphthalene dianhydride) proved to be very difficult, as there was only one paper documenting such a synthesis [35]. This was compounded by the fact that the paper was somewhat unreliable with vague measurements and titration procedures that failed to meet produce the desired material, hence the improvised additional steps mentioned in the experimental section. Once the first group was attached though, adding the second tail was rather easy.

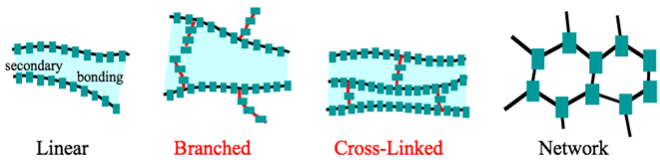

Figure 23: Polymer Structures [32]

In the end we managed to synthesize NTCDA (NMR spectra is shown in the Appendix), but the problems encountered can be overall attributed to pH sensitivity of the reaction. As pH is a logarithmic scale, it was thought that it would not difficult to hit the 6.5 and 6.3 pH values. In terms of percentage about 60% extra acid or base would need to be added to over or under shoot these values, a rather significant quantity. Using 10% excess of the chemicals was supposed to ensure the desired reaction took place and the fact that phosphoric acid would create a buffer solution would have also aided it easily reaching the required pH values.

However, while the numbers worked out well on paper in reality that was hardly the case. For example, depending on whether the phosphoric acid was assumed to transfer either 2 or 3 of the possible H^+ ions had a large impact on the calculated values. Additionally, in the first synthesis attempts the pH was measured with paper indicator strips, so the measurement lacked precision. In hindsight, the reason the original synthesis paper might have been left intentionally vague in some areas is because working out the numbers on paper does not necessarily lead to an exact synthesis. In this project following the calculated measurements were usually found to overshoot the pH values, which led to solutions which either precipitated too early or failed to precipitate at all.

In the end, the solution led to a successful precipitation at pH 6.5 opposed to 6.3. Since the potassium hydroxide is simply used to open up the ends of the naphthalene dianhydride, only a minimum amount of phosphoric needs to be added to neutralize the remaining OH^- ions. Taking a 10% excess is most likely not necessary and an acceptable pH at this point could probably higher than the proposed 6.5. More importantly, using a calibrated pH meter and adding solutions dropwise are far more critical factors to a successful reaction than knowing the exact quantity of a certain chemical to add for this synthesis.

Also, following this improved synthesis route may improve the yield and remove the need for purification by recrystallization. In all of the synthesis attempts, even the successful one, there was always some of the original starting compound or a naphthalene with both sides functionalized. Getting rid of these led to material losses and additional processing steps which were not reported as necessary in the original paper. Avoiding these extra hindrances would improve the synthesis plan.

During this synthesis as it was becoming more apparent how time consuming NTCDA was to make, it was decided to synthesize another version of NTCDA as backup. In the event of a failure in making the ideal NTCDA or PNTCDA, at least there would be some material of a similar nature for cell testing. This version of naphthalene diimide had a butylamine tail on both sides and therefore the synthesis was rather straightforward. It followed the plan of Matsunaga et. al. which was quite easy and fast [27]. However, this material was already known to be soluble in organic electrolytes, hence why the goal was to make a polymer [3]. Naphthalene diimides with different functional groups than those used here have been found to be soluble in water as well, but since it was not known whether or not this version would be soluble in water it would at least be useful for aqueous testing [56]. As per the results of the polymerization in the following section, it was this naphthalene diimide henceforth referred to as ND, with butylamine tails that had to be used for the cell tests.

5.2.2 Polymers

Unfortunately, the polymerizations were a bit of a disaster. As previously explained, the NTCDA synthesis did not go according to plan and when the purified material was finally obtained there was only roughly 0.6 g remaining corresponding to a 25% yield from start to finish. While this was enough to polymerize, it turned out to be insoluble in dichloromethane and thus failed to react with the acrylate. According to literature regular naphthalene diimide is soluble in dichloromethane as well as many other organic solvents, so either not enough solvent was used or the functional tails reduced the solubility of the compound [1]. The anthraquinone and naphthalimide both ended up getting contaminated with air, which impeded the reaction. This is considered to have occurred when the pyridine and poly acryloyl chloride were added as a quick flare of dark smoke appeared, which was unexpected.

Fortunately, all the compounds were able to be recovered by extraction, but in the process the losses of NTCDA left only 350 mg, which was not enough to attempt a second polymerization. The anthraquinone and naphthalimide were successfully recovered in large enough quantities to attempt the polymerization again, yet on a smaller scale. This time a rubber gasket was used in the flasks when adding solutions and the pyridine, poly acryolyl chloride, and methanol were pulled from their bottles under argon to ensure minimal possibility of air contamination. This time poly naphthalimide was successfully synthesized, but the anthraquinone remained in solution.

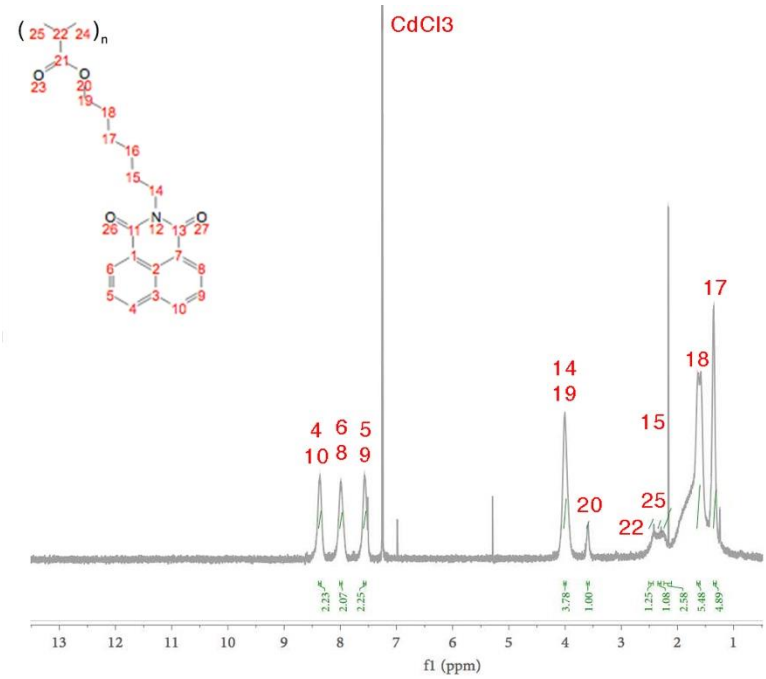

Figure 24: Poly-naphthalimide NMR

Since none of the materials have ever been made before it is still rather promising to know that at least naphthalimide can be made into an acrylate branched type polymer. As only 90 mg was made it was enough for NMR, but not enough for any kind of cell testing. The NMR spectra indicated a grafting degree of roughly 70%, so the highly anticipated problem of cross linking was not an issue. If anything more acrylate should have been used in order to polymerize the the naphthalimide that remained in solution. As for the anthraquinone, it is highly suspected that the powder contained a high degree of moisture despite being in a heated vacuum oven for 24 hours before polymerization. As a result, the acrylate formed a large cross-linked mess while the anthraquinone failed to react. For these reasons, as well as the fact that after two extractions to recover the material the purity was degraded, anthraquinone was not considered for any testing.

5.2 Half Cell Testing

In this section the results of the half cell tests against pure sodium metal in organic electrolyte are presented. The purpose of these tests is to ensure expected and desirable material performance in half cells before continuing onto full cell testing. Any problems encountered in these tests can be attributed to fewer factors as there are fewer variables involved and therefore identifying and isolating problems should be easier. Once the materials' electrochemical performance is proven we can then move forward to full cell organic testing.

5.2.1 $Na_{0.44}MnO_2$

The first test carried out for $Na_{0.44}MnO_2$ was to confirm the results found in literature, so the electrode was tested in the same 0.8 V range. The (dis)charge curve profiles match those found in literature and over the course of 20 cycles 93% of the theoretical capacity was achieved. These results were well within the stability window of water (~ 2 - 3.7 V) indicating stable performance that should be reproducible in aqueous cells.

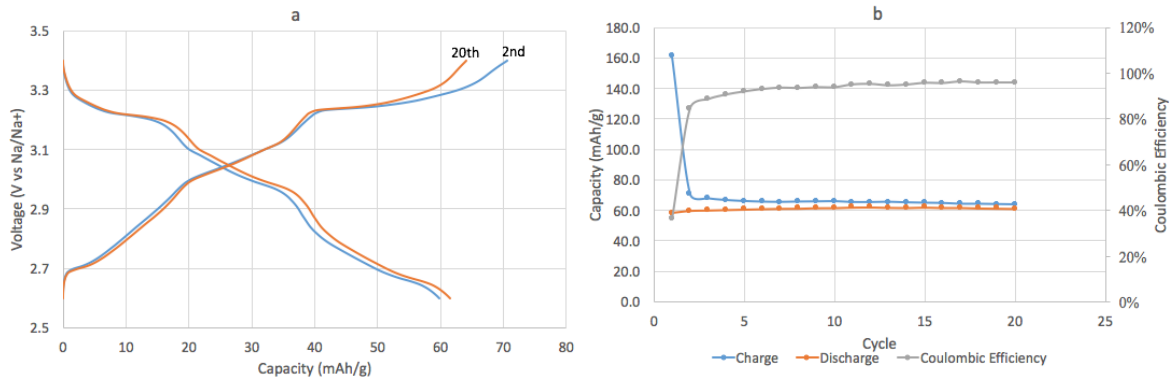

Figure 25: a. (Dis)Charge Curves b. Cycle Chart for $Na_{0.44}MnO_2$ at 0.1C Rate

The same test was then repeated, but in a 2.5 V range encompassing the stability window of water. The voltage range selected was actually slightly larger than the stability window, however this would show the performance in the event of large overpotentials in the aqueous cell. While the material did function it ended up achieving capacities much higher than the theoretical maximum. This indicates a phase change from $Na_{0.44}$ to Na_x where $x > 0.44$. A rough estimate by reversing the capacity calculation indicates $x = 0.57$, which would correspond to a 46% increase in sodium ion intercalation. Since the sodium metal is an unlimited sodium ion source the extended voltage range allowed for more sodium ions to intercalate. The structural changes accompanied by the additional sodium ions seem to degrade the material. Over many cycles the specific capacity severely decreases somewhat stabilizing as it dips below the practical maximum. Since the structural changes accompanied by additional sodium ions negatively impact the crystal structure the material ends up slightly underperforming compared to when kept within a more reasonable voltage window, yet still delivers a relatively normal capacity.

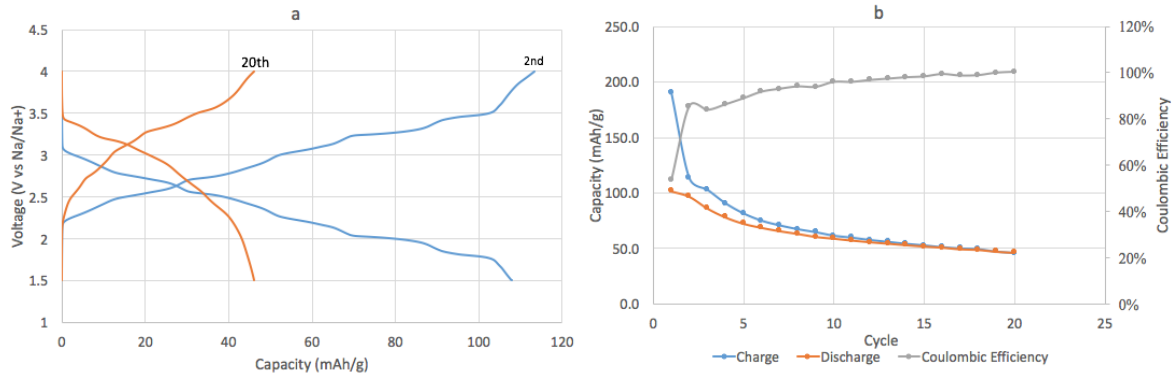

Figure 26: a. (Dis)Charge Curves b. Cycle Chart for $Na_{0.44}MnO_2$ at 0.1C Rate

The last tests were to determine the long term cyclability of sodium manganese oxide within the same two voltage ranges previously used. When cycled within the range used in literature only 45% of the theoretical capacity was achieved, yet it was consistently maintained for 200

cycles. The underwhelming performance may be attributed to the high C rate used, which forces faster reaction kinetics and increases internal losses. The material's specific capacity has shown to decrease with an increasing C rate and the resulting capacity here is actually slightly higher than what is reported for 0.1C tests [48]. Conversely, the material shows much higher capacities when cycled at 1C in a wider voltage range. Considering that the capacity always remains above the theoretical maximum it implies that the material over-intercalated sodium, but managed to remain in a metastable form somewhere between $Na_{0.44}$ and $Na_{0.57}$.

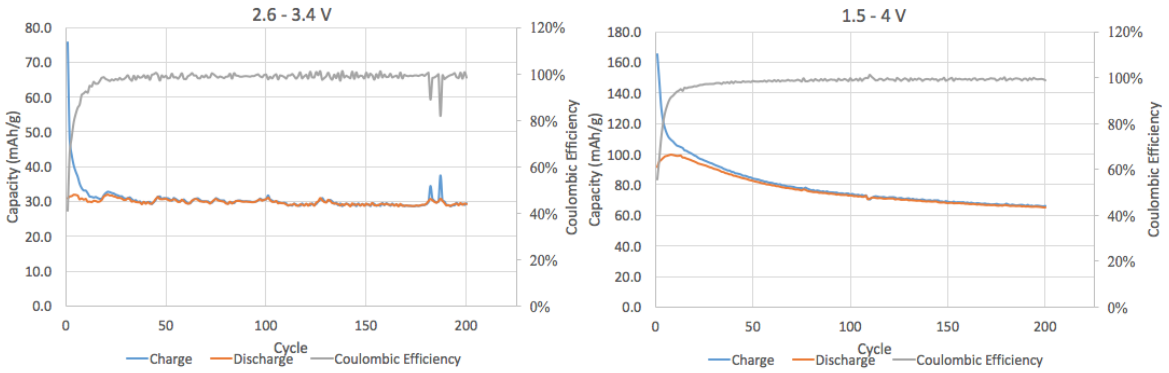

Figure 27: Cycle Charts for $Na_{0.44}MnO_2$ at 1C Rate

Overall these results indicated that $Na_{0.44}MnO_2$ performs ideally when kept within a smaller voltage window. While it can deliver comparable capacities in wider voltage windows it is due to additional sodium ions which intercalate and deteriorate the material over time. In a full cell this may lead to more severe electrode damage as there will not be an infinite sodium source as a counter electrode.

5.2.2 $Na_{0.66}MnO_2$

There has been little testing of $Na_{0.66}MnO_2$ or sodium manganese oxides of a comparable sodium content at the time of writing. Due to the lack of previous studies and unfamiliarity with the material the first tests conducted used the same settings as the $Na_{0.44}MnO_2$ tests. Unfortunately, the results were lackluster. While the material displayed readily reversible (dis)charging and good cycle stability the capacity was small, even compared to that of $Na_{0.44}MnO_2$. There was also significant irreversible capacity loss in the first cycle attributed to the removal of extra sodium, which was not able to be reversibly inserted.

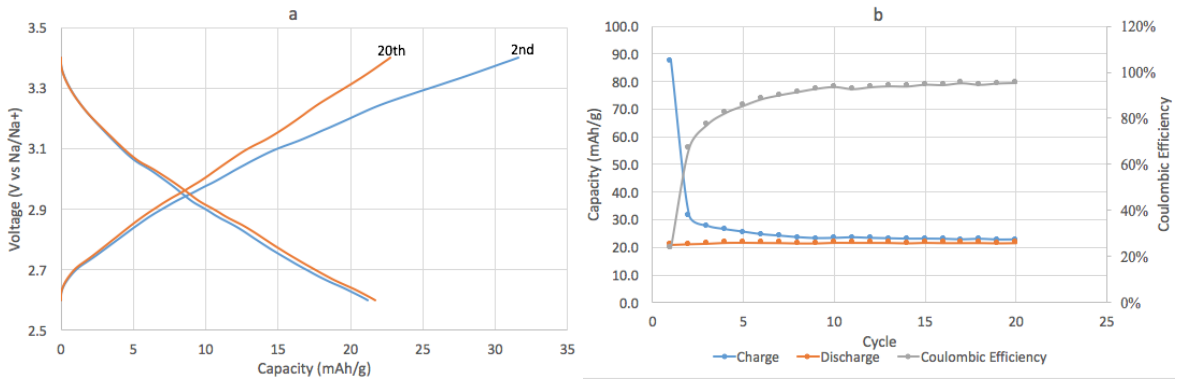

Figure 28: a. (Dis)Charge Curves b. Cycle Chart for $Na_{0.66}MnO_2$ at 0.1C Rate

One possibility was that the voltage window was not wide enough to encompass the full charge curve as in the plot above it has clearly yet to show signs of a steep slope normally associated

with completed charging. Nevertheless, when tested in a 2.5 V range the results were similar. While the capacity was significantly improved it was still about 67% of the theoretical maximum after 10 cycles and there was a good degree of capacity fading. The initial cycles did obtain the theoretical capacity, but this was only briefly maintained.

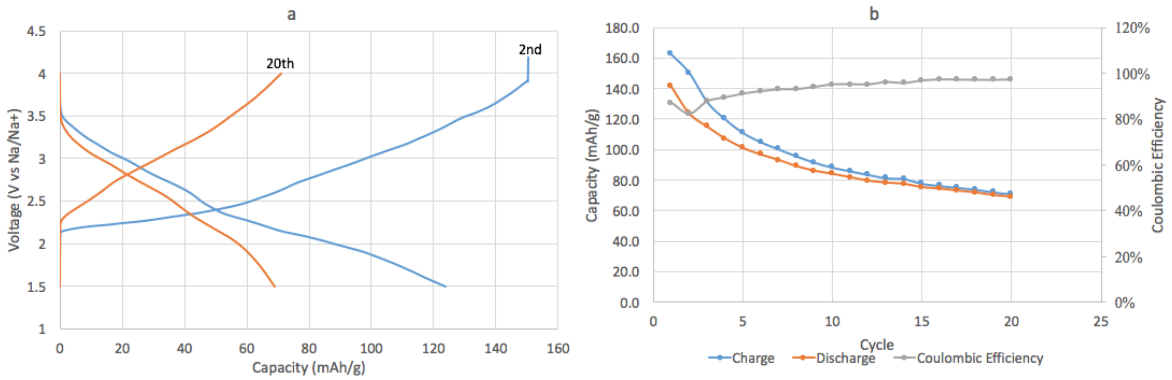

Figure 29: a. (Dis)Charge Curves b. Cycle Chart for $Na_{0.66}MnO_2$ at 0.1C Rate

When the same tests were repeated at a 1C rate for 200 cycles the capacities were lower as expected, yet showed some signs of stabilization after about 50 cycles. Regardless, the capacities were still lower than those of the $Na_{0.44}$ thus indicating no discernable advantage over the other phase despite the higher initial sodium content, which was unlike literature [40]. It was actually quite unusual considering that in the case of the $Na_{0.44}$ phase there were points where extra sodium is intercalated, so it was even expected that the same occurrence might happen here and push the material capacities higher than the theoretical maximum.

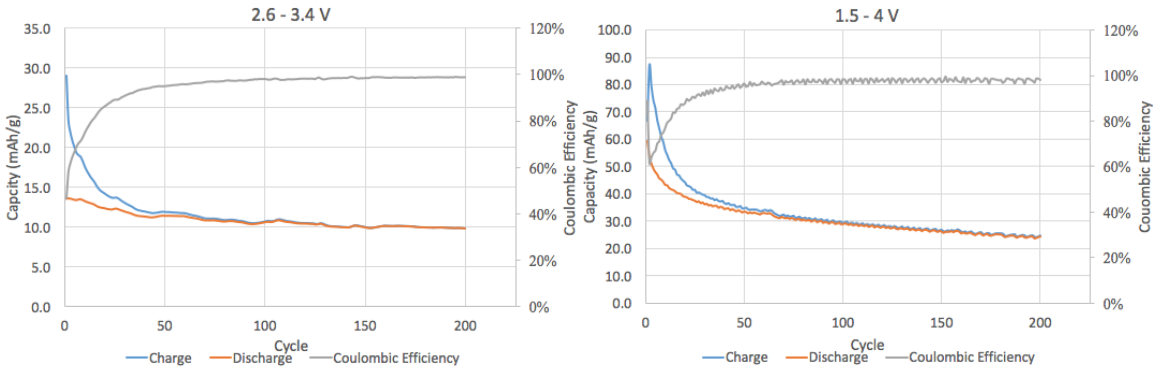

Figure 30: Cycle Charts for $Na_{0.66}MnO_2$ at 1C Rate

In testing the same material as an electrode against lithium higher capacities are reached, yet this is not an ideal comparison as when cycled against lithium the lithium intercalates into interstitial sites of the birnessite structure whereas versus sodium the sodium itself is removed from the crystal lattice [52]. Therefore, one possible explanation for the poor performance is the greater stress on the crystal structure as more sodium is intercalating into and out of the lattice. Yet given the number of metastable phases of different sodium contents, this is unlikely the case.

In order to gain more insight into the behavior additional tests were conducted within an intermediate 1.4 V range (2.3 – 3.7 V), which is shown in the Appendix. A similar performance was realized again with significant first cycle irreversible capacity loss, but minimal capacity fading over cycling. Considering the material is capable of reaching its theoretical capacity in

the first cycle but not thereafter, it seems to be that the minimum value of sodium content is not $Na_{0.2}$ as it is with $Na_{0.44}MnO_2$ [7]. If it were the case, the first cycle capacity would be maintained throughout, but instead the minimum sodium content in the charged state must be higher. In fact, a much more likely hypothesis is that regardless of the initial sodium content only about $Na_{0.24}$ is migrating at any given time.

This can be shown in the graph below where the amount of sodium ions per $Na_{0.66}MnO_2$ molecule are shown alongside the cycle chart. Larger potentials are required to extract the sodium and even then the same amount of sodium is transferred compared to $Na_{0.44}MnO_2$. Only in the largest potential window can the majority of the sodium be fully extracted and it cannot maintain this performance.

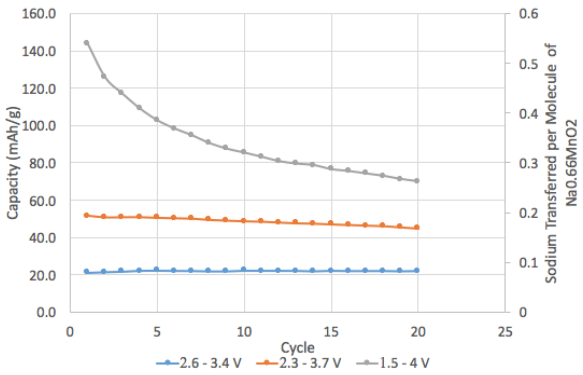

Figure 31: Sodium Transferred per Molecule of $Na_{0.66}MnO_2$ at 0.1C Rate

Based off of the results of Doeff et. al. it was presumed that $Na_{0.2}$ would be the minimum sodium content for all sodium manganese oxides, even though it was only confirmed for $Na_{0.44}MnO_2$. If instead viewed from the perspective that only 0.24 sodium ions are migrating per molecule for all sodium manganese oxides, then the results presented here line up with the expected theoretical capacity. Under this premise though there is no advantage of using higher sodium contents, as the amount of sodium transferred remains constant. If anything there is a weight penalty for higher sodium contents because the transferred amount stays the same, so the remaining sodium in the manganese oxide provides dead weight lowering the specific capacity. This idea is further supported by a paper finding that for α and β phases of manganese oxide with 0.4 and 0.7 sodium contents, only a fixed amount of sodium can be reversibly inserted and it does not necessarily scale with larger starting sodium content, nor does it improve long term cycling stability [38]. Tevar et al. only saw a 30% capacity bonus from going from a $Na_{0.44}$ to $Na_{0.66}$ phase, which is far below the expected gain and their results still underperformed compared to these new findings [40].

In the end further testing could yield a potential range and current rate that optimize the $Na_{0.66}$ phase or other sodium manages oxides for more sodium extraction, however that became outside the scope of this project. Ultimately, $Na_{0.66}MnO_2$ could yield an acceptable capacity, but much lower than expected and with degrading performance over extended cycling. Due to these detriments it provided no apparent benefit over the $Na_{0.44}MnO_2$ phase and was no longer considered for use in full cell testing.

5.2.3 λ-MnO_2

The spinel manganese oxide was one of the more interesting materials to work with due to its unusual behavior. Since it was a material previously well researched in literature the

expectation was that testing would be a straightforward confirmation of functionality as it was with $Na_{0.44}MnO_2$, yet this was not the case. In early tests it was difficult to make a half cell that could achieve more than 10 mAh/g despite adjusting the the current and voltage range.

Eventually after trying some longer cycling tests, despite the poor initial results, there was a strange occurrence. The capacity was actually increasing over time. Based on the voltage profiles in the first cycles it is safe to say there is no intercalation, but rather a more capacitive behavior corresponding to interactions at the phase boundary between the electrode and electrolyte. The profile becomes more defined over time eventually displaying a visible plateau. This behavior was observed in many tests and as cycling continued it would slowly reach a maximum capacity near 100 mAh/g before slowly degrading.

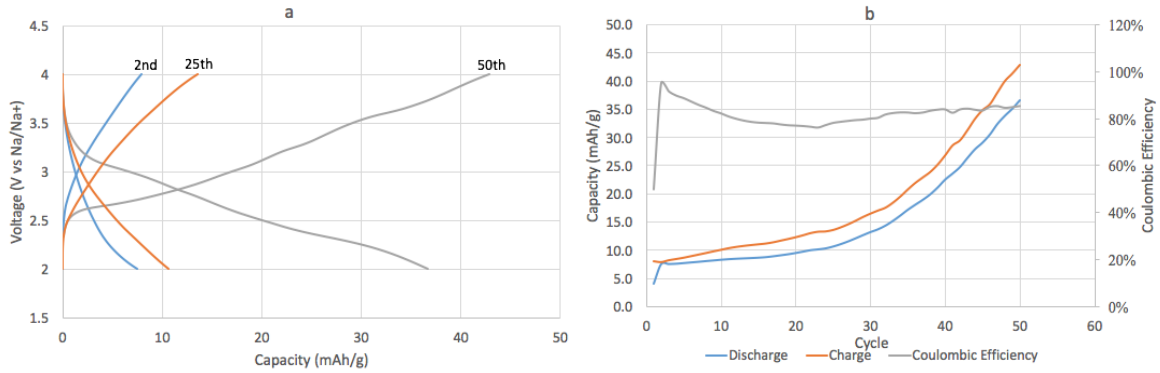

Figure 32: a. (Dis)Charge Curves b. Cycle Chart for λ-MnO_2 at 0.1C Rate

At first it was thought that perhaps the coating could be causing the strange effect. Changing the test settings had little to no effect and since the synthesized lambda phase material was completely pure the only way it could have been affected was during the coating process. Therefore several different coatings were made with changes to the thickness, pressing to decrease porousness, and an attempt to decrease the particle size. These variations still yielded an S shaped curve having only changed the rate at which the capacity increased and the rate at which it degrades after hitting its peak. Two of these results are shown in the Appendix. At this point it became apparent that something was happening with the material itself.

Manganese oxide can come in many forms, so the next hypothesis was that there was a phase transition during cycling that affected the performance. Fortunately, there was already a study about the different phases of manganese oxide and their respective energies alongside sodium content. Using DFT methods they were able to find that for low sodium contents the alpha phase of manganese oxide was the lowest metastable phase [21]. Based off of the capacities in previous tests it was clear that far less than the expected amount of sodium was being inserted, which is why the sigma phase was not considered. In order to verify this XRD measurements were taken of the electrode after 2, 50, and 200 cycles. These are shown compared to the starting lambda phase and alpha phase in Figure 33.

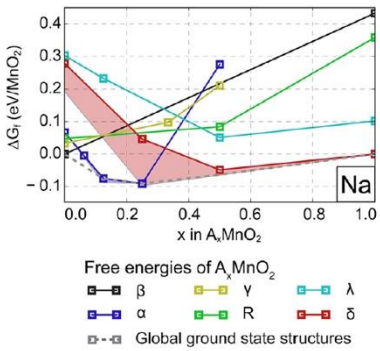

Figure 33: Free energies of manganese oxide by phase and sodium content [21]

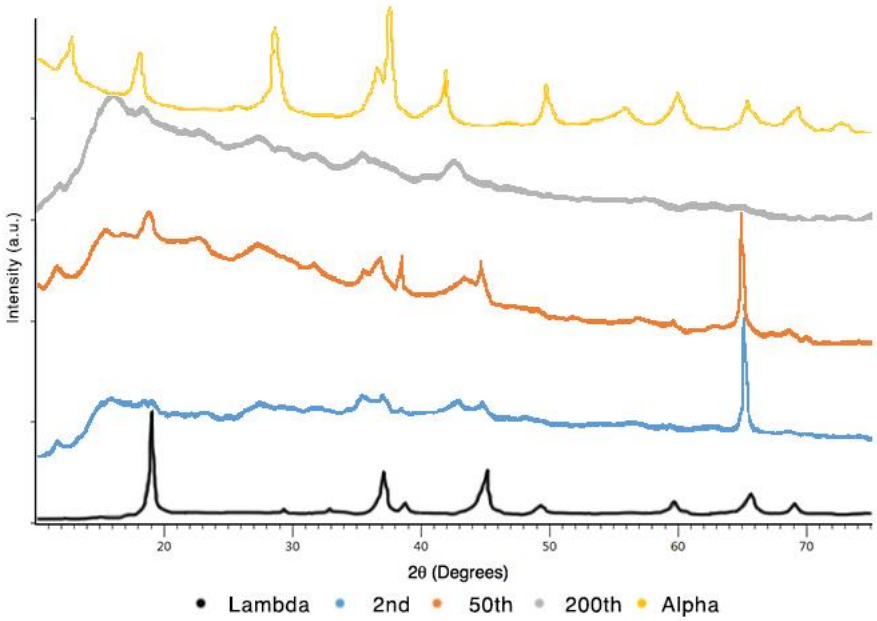

Figure 34: XRD of Positive Electrode at Various Points in Cycling Compared to λ and α MnO_2 Phases [54]

Based on the results it seemed that the spinel phase is destroyed upon first insertion, yet by the 50th cycle at which point the material obtains its highest capacity the phase was ever present. From there on out it gradually degraded until it was virtually amorphous. One paper on manganese oxides claimed a phase transition from a lambda phase to a monoclinic crystal in which cells obtained capacities of 200 mAh/g. However, this performance was only demonstrated for short tests (10 cycles), so this was certainly not what was happening here [50]. The first cycle capacity loss indicated a high amount of sodium insertion, which never occurred again even after the material regained the lambda phase at the 50th cycle. Naturally inserting one sodium ion per MnO_2 would be ideal, however more common ratios are closer to 0.6:1 for Na:MnO_2. This was shown in the first cycle in many of the tests, however once the material stabilized a smaller amount of sodium was actually being reversibly inserted. Some phenomena in the first cycle caused irreversible sodium insertion, which appeared to leave a sort of λ phase Na_xMnO_2 structure. Normally these kinds of crystals are α or β phase birnessite structures [38]. Regardless, it was clear that the new crystal structure could easily host 0.3 Na

ions per Mn, which was a significant gain (30% increase in mAh/g) over the previously tested sodium manganese oxides.

In a final attempt to achieve stable and high capacity performance with the λ-MnO_2 a test was conducted with a reduced voltage window. When cycled in a sufficiently small potential range the material never phase changes and maintains low capacities throughout cycling. Therefore, the material was cycled in the normal 2 – 4 V range and then at cycle 50, which was usually where the peak occurred, the voltage window was then reduced to 2.25 – 3.75 V. Hopefully keeping the range strictly within the voltage plateau would eliminate long term cycling degradation and the peak capacity could be maintained in extended cycling. This result was then plotted against the performance of a same cell that maintained the original potential range throughout.

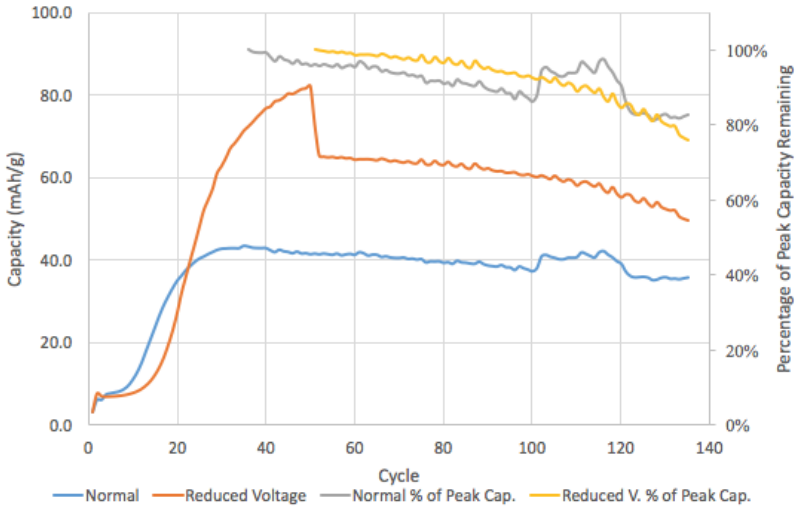

Figure 35: Comparison of Regular and Reduced Voltage λ-MnO_2 at 0.1C Rate

Unfortunately, these results were disastrous for three reasons. Firstly, one test had to be stopped before the full 200 cycles due to Maccor maintenance, which is why they are only plotted to the 135th cycle. Secondly, the cell which cycled in the normal potential range had an abnormally small amount of active of material on the electrode, so the values of the capacities could not be compared in absolute terms. Then in order to try to draw a conclusion the remaining capacities were plotted as a percentage of the peak capacity. This led to the third issue being that when the normal cell was cycling around cycle 100 – 120 there was an unusually hot 30° C weekend during which the air conditioning in the test room broke down leading to an increase in temperature. This led to higher conductivity and thus high capacities, which further hinder comparisons between the data. Ultimately it appears that by forgoing some extra capacity by reducing the voltage range, extended cycling degradation can be slowed. Nevertheless, due to the complications in the data set there is not much confidence behind this without repeating the tests under better conditions.

Lastly for use in a full cell the material would have to be pre-sodiated by cycling it once against sodium and then extracting the electrode and placing it in a new cell. While this was possible and successfully executed, it was time consuming and very labor intensive, making it a cumbersome process for a material with irregular behavior. Therefore, it was no longer used.

5.2.4 ND

Given the results of the polymerization the aforementioned ND with butylamine tails was then used for cell testing. Naturally it was expected that the material would dissolve into the electrolyte as reported in literature [45]. Unsurprisingly this is what occurred. The material was able to be reversibly sodiated, but with significant permanent capacity loss in each subsequent cycle. Even in the initial cycles the material does not come close to reaching its theoretical capacity of 284 mAh/g. Occasionally higher capacities around 45 mAh/g were reached in the first cycles, but this was never maintained and then the dissolution rate was even faster.

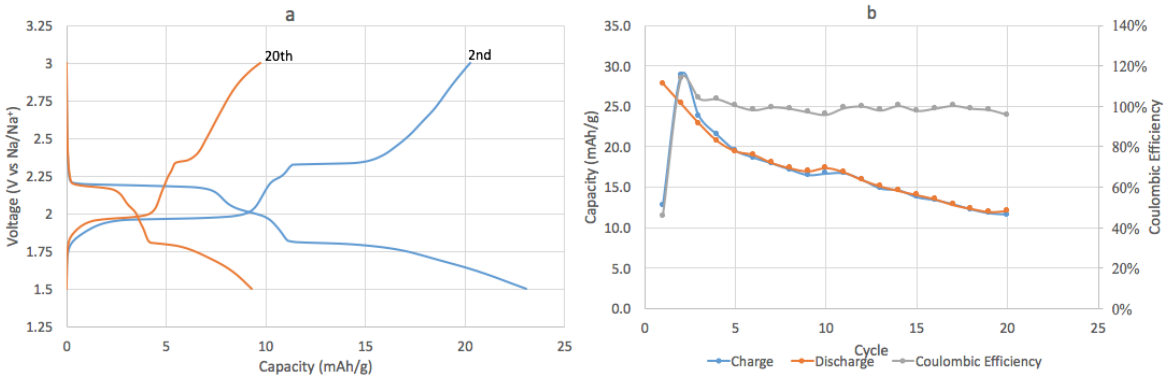

Figure 36: a. (Dis)Charge Curves b. Cycle Chart for ND at 0.1C Rate

The greatest point of interest in these plots is the clear display of two voltage plateaus. In almost all literature on this compound in sodium half cells it is only said to have one plateau corresponding to two sodium ions on opposite sides of the molecule. In these tests it appears that all four possible bonding sites host a sodium ion, which is also what was previously anticipated in literature, yet never achieved. This means that the materials theoretical capacity could actually be 284 mAh/g as most papers now calculate the theoretical maximum based on the bonding of only two sodium atoms.

The only key difference is that in literature this material is tested as a linear type polymer and here it was tested as a monomer. It is proposed that the organized and close spacing of the polymer provides some additional electric repulsion between the oxygen atoms, which requires discharging to below 1.5 V in order to fully bond all four sodium atoms. However, this comes with structural damage to the electrode material, not to mention going even further out of the stability window for water. However, as a monomer both plateaus occurred above 1.5 V, indicating that the reversible full capacity can be realized in a cell. Although for this to be achieved measures other than polymerization must be taken to mitigate solubility problems as polymerization impedes the total 4 electrons from transferring [3][45].

Overall the capacity was disappointing, but given the solubility issues this was no surprise. Given the cyclability and performance it was worthwhile to go forward and test this material in a full cell. Being an organic compound it would not be useful to XRD the anode to verify the sodium content, however in future research it may be worthwhile to use solid state NMR to check this result.

5.2.5 Naphthalimide

Since raw naphthalimide has never been tested as a battery material, the initial half cell tests were conducted in the same voltage range as the other anode materials. As they all have similar base structures, benzene rings with oxygen double bonds, it seemed likely that the voltage

plateaus would fall in the same range. While this did seem to be the case the electrochemical behavior of the material was not as desired.

When first assembled the cell already measured a voltage lower than 1.5 V, which was the lower voltage limit for charging. Therefore when the test started it immediately registered as finished charging and continued into discharging where 122% of the theoretical capacity was achieved in the first discharge shown in Figure 37. Immediately afterwards the cell would no longer transfer sodium as the capacity dropped to 8 mAh/g in subsequent cycles.

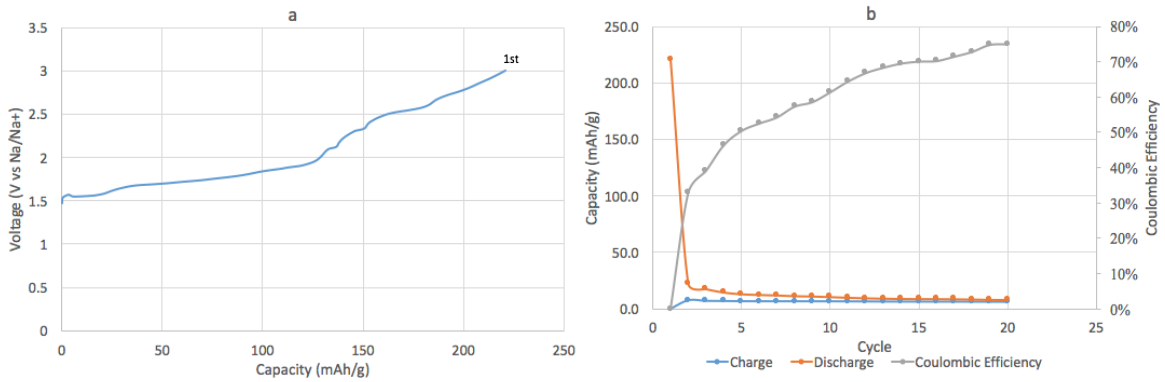

Figure 37: a. Discharge Curve b. Cycle Chart for Naphthalimide at 0.1C Rate

The immediate loss in functionality after the first cycle made it appear as if solubility was not a mechanism for loss of capacity in this cell. Additional tests in alternate voltage ranges were conducted, where it was sometimes possible to obtain reversible capacities around 25 mAh/g, but even this would only be maintained for three cycles before the cell died. Also, lowering the voltage limit to 1 or 0.5 V was already way out of the stability window of water, so even if the full capacity was reversible in this range it would not be usable in an aqueous cell.

It is highly suspected that the problem encountered here is attributed to the functional hexanol tail. Ideally sodium can only bond with the two free oxygens, however the OH at the end of the tail offered another bonding site with adverse effects. The OH single bond has a bond disassociation energy of 428 kJ/mol which is significantly lower than the 749 kJ/mol required to break the double bond between C and O [37]. Thus it is more energetically favorable for sodium to bond at the tail, which would leave free hydrogen ions. This idea is supported by the fact that over 100% of the theoretical capacity is obtained, which most likely comes from additional sodium bonding at the tail of the molecule. Given that the counter electrode was pure sodium metal, it would be impossible to consume all the sodium if for example, the free hydrogen ions were bonding with sodium to form sodium hydride. Therefore, it seems likely that another reaction is taking place at the oxygen sites, which permanently blocks sodium from bonding there.

5.3 Full Cell Organic Testing

With the materials tested in half cells, the next step was to see if the electrochemistry still worked in a full cell with organic electrolyte. If this step proved to be successful then the cell would be considered for aqueous testing. The goal was to build up they system to a full aqueous cell changing as few variables between each testing phase.

5.3.1 ND/$Na_{0.44}MnO_2$

When finally testing the ND vs $Na_{0.44}MnO_2$ the cell was capable of delivering reasonable capacities during cycling. Naturally there was still a lot of electrode dissolution at the anode side, as evidenced in the declining capacities shown in the plot below. While the capacity fading was pronounced, in initial cycles 35% of the theoretical capacity was achieved and ideally without dissolution problems the percentage would be much higher. It was promising though to see charge profile as it clearly indicates full electrochemical function in both materials. The plateaus starting at 0.8 and 1 V are attributed to the ND, yet are less flat due to the curve of $Na_{0.44}MnO_2$ and the last shoulder at 1.2 came from the discharge of $Na_{0.44}MnO_2$.

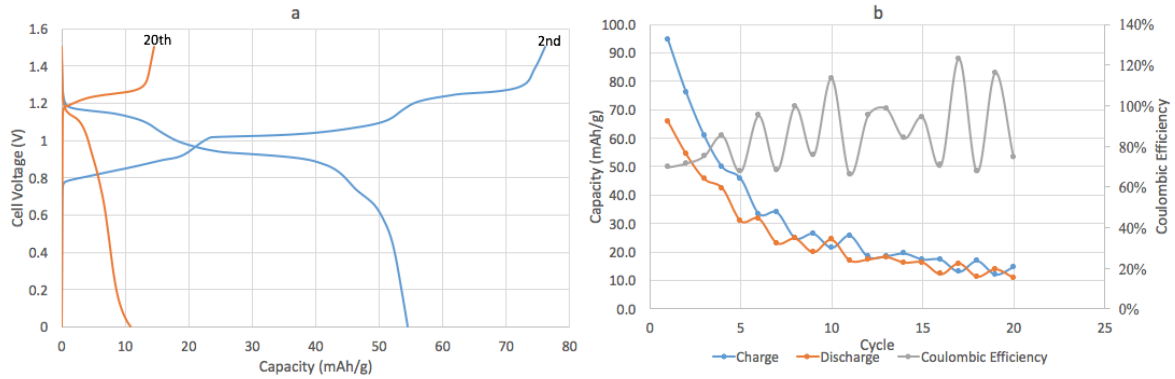

Figure 38: a. (Dis)Charge Curves b. Cycle Chart for ND vs $Na_{0.44}MnO_2$ at 0.1C Rate

One oddity remained that the cell achieved higher capacities than in the ND half cell test. Given that the electrodes had the same thickness coating, the $Na_{0.44}MnO_2$ electrode was oversized as to overcompensate for ND larger specific capacity. This way ND would be the rate limiting electrode. In tests where there was a severe size difference between the electrodes the cells did not work, which is most likely because in reality only the small area of the cathode that overlapped with the anode was actually transferring ions back and forth. Thus, slightly larger anodes had to be used, which then made the cell cathode limited. With an excess of ND it would be possible for some to dissolve, yet still leave a sufficient amount on the electrode to achieve higher capacities than in the half cell test.

Once again, the dissolution issue encountered was expected. Given the reasonable capacitates and possibility that dissolution might not be a problem in an aqueous cell it was decided to attempt cycling this cell in the aqueous setup.

5.3.2 Naphthalimide/$Na_{0.44}MnO_2$

Despite the dismal results of the naphthalimide half cell tests, an attempt was made to cycle the material in a full cell. Perhaps with a different cathode the inhibiting reaction might not occur. However, this was not the case as the cell reached a capacity 1.5 times the theoretical maximum. This value is by no means coincidental as it indicates that sodium was indeed bonding at the tail in addition to the two double bond sites intended.

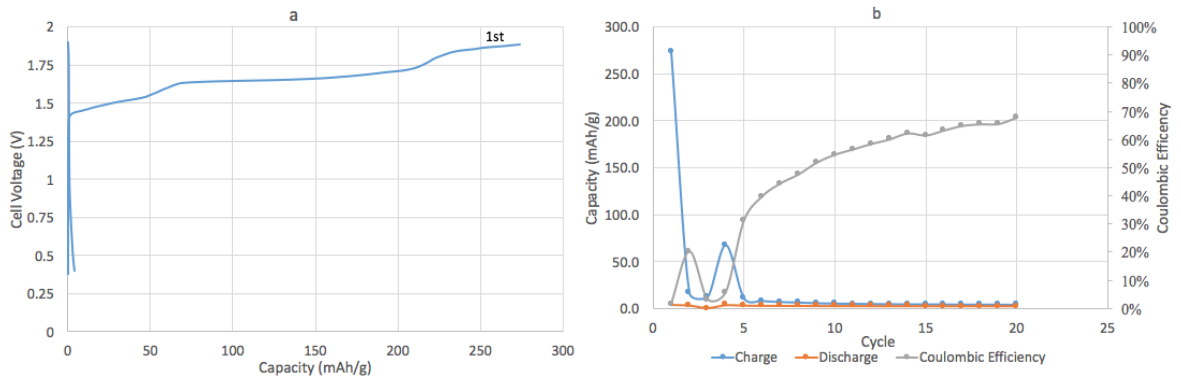

Figure 39: a. (Dis)Charge Curves b. Cycle Chart for Naphthalimide vs $Na_{0.44}MnO_2$ at 0.1C Rate

Without further investigation, perhaps by solid state NMR, it is difficult to tell exactly what is happening. Yet it remains clear that some unintended reaction most likely attributed to the function OH group is blocking sodium transport or at the very least rendering the reaction irreversible. Without resolving this issue there was no point in taking this to the aqueous setup.

5.4 Full Cell Aqueous Testing

Based on the previous results only one chemistry seemed to display potential that it might be functional in an aqueous cell. This was the ND/ $Na_{0.44}MnO_2$ full cell.

5.4.1 ND/$Na_{0.44}MnO_2$

Testing this material combination in the aqueous cell did not come close to reproducing the performance observed in organic electrolyte. There seemed to be no overpotentials, so right away at 1.23 V the water would begin to split and the voltage range had to be capped much lower than expected. Furthermore, the half cell potentials showed no signs of their regular plateaus, not to mention the capacity achieved was insignificant. During the discharge, the voltage simply dropped indicating no desired electrochemical effect taking place. After observing this behavior, the same test was conducted with the half cell voltages allowed to flip. This too did not seem to make a difference. Given the insignificant capacities achieved, it is difficult to ascertain any real information from these charts.

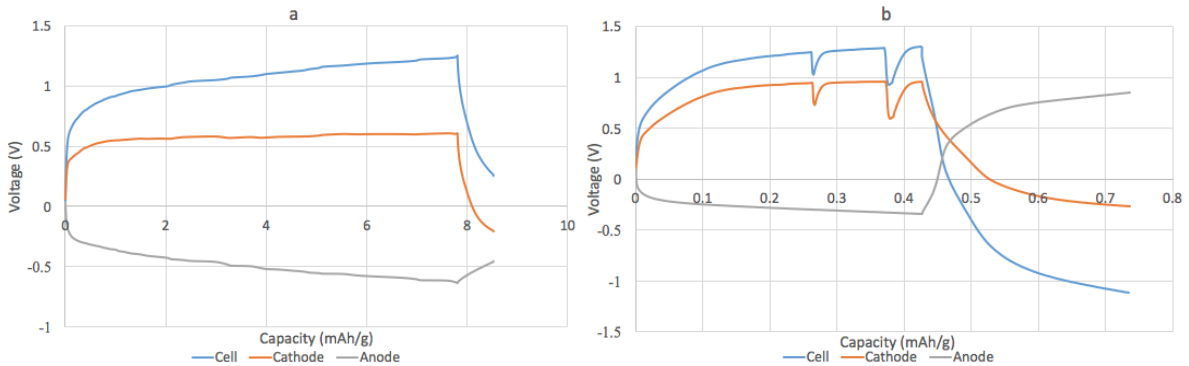

Figure 40: (Dis)Charge Curves for ND vs $Na_{0.44}MnO_2$ at 0.1C Rate
a. 0 – 1.25 V b. -1.25 – 1.25 V

Due to the difficulty in obtaining optimistic results in the aqueous setup, an attempt was made to assemble an aqueous cell in the standard Swagelok cell. The major disadvantages of this

approach were that the cell would contain air and not be able to measure half cell potentials. However, this was a worthwhile concession as the cell was able to charge to its full capacity. Even without seeing the half cell potentials the overall profile of the curve greatly resembled the curve seen in the organic test. The slight differences can be attributed to the fact that a different test procedure was used. In the interest of time an additional condition was added to the test. It was set to cycle between -1.25 and 1.25 V, but would also switch if the (dis)charge time exceeded 10 hours. As seen in Figure 41a the charge does not reach the 1.25 V limit, but as it had been charging for 10 hours it switched to discharging. This is most likely why such a high coulombic efficiency is achieved. If simply allowed to cycle between the voltage limits, it seems the the charge curve could continue onwards, while the discharge curve nearly hits the voltage limit in the same amount of time. Only the first three cycles are shown because at the time of writing the cell was still cycling.

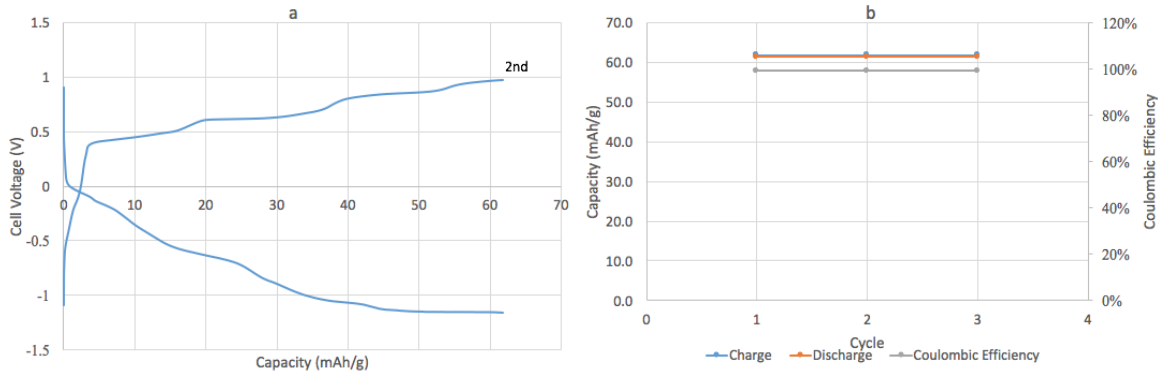

Figure 41: a. Charge Curve b. Cycle Chart for ND vs $Na_{0.44}MnO_2$ at 0.1C Rate

Given that the cell achieves its theoretical capacity with good reversibility, it seemed that the materials functioned well. However, due to the difficulty in coating carbon cloth with the appropriate mass loadings the test was by no means anode limited, making it not an ideal representation of the full functionality of ND, which was the material of interest. Despite the good performance it was strange that the cell had to be cycled to negative potentials to be reversible. Considering the reversible capacities achieved it seemed the desired reaction was taking place, although longer cycling may reveal fading which could be caused by a variety of reasons, such as side reactions or electrolyte decomposition. However, given the current results and the assumption that this performance is maintained it is more likely that the severe overpotentials came from gas buildup or the alternative reaction mechanism of the negative electrode.

It is possible for water to split below its theoretical potential, which may occur leading to gas buildup in the cell causing overpotentials. When the charging is completed and the current is reversed the voltage relaxes due to the loss of internal resistance and these bubbles could then dissipate accounting for the large voltage drop. Additionally, most batteries rely on intercalation to store charge, but for this organic material chemical bonding is the mechanism for storage. This mechanism may lead to more energy being required to break the bonds and transport sodium. Not to mention, the presence of water may exacerbate this issue and the dissolution of anode material into the electrolyte might have masked these problems in the organic half and full cell tests.

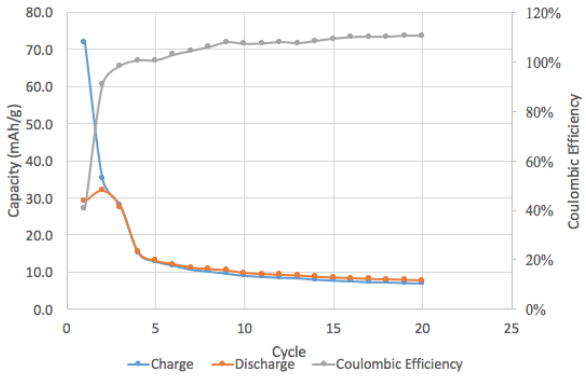

Figure 42: Cycle Chart for ND vs $Na_{0.44}MnO_2$ at 1C Rate

Lastly, the same test was conducted at a 1C rate where the high current forced faster reaction kinetics, which lead to the removal of more than 0.24 Na ions per manganese oxide. This is made clear by the initial charge reaching a capacity higher than the theoretical maximum. The removal of additional sodium from the cathode must have caused electrode degradation as previously shown in the sodium manganese oxide half cell tests. This is likely what led to the loss in irreversible capacity loss until the material stabilized reversibly cycling about 10 mAh/g. Ultimately the C/10 rate results were quite optimistic and further testing is needed to confirm whether this performance can be maintained for long enough to be truly significant. Also the material did not dissolve in aqueous electrolyte which was ideal.

6 Conclusions and Recommendations

Finally, in this chapter some closing thoughts are given about this project work as well as some suggestions for future research on this topic. While overall it was difficult to obtain the final goal, there is still a lot to be learned in the process and these insights can be used to proceed faster and more efficiently in ongoing experimental work.

6.1 Synthesis

In the end only one of the three polymers was successfully made, yet even so it was in too small a quantity to test in a cell. It seems likely that all three could be made given more time to prepare an excess of starting compound in order to give the polymerization multiple attempts. This would allow for the process the be refined and then greater yields could be achieved in less time. Regardless, the success of the poly-naphthalimide synthesis shows that this form of polymerization can be a viable method to create novel organic polymer anodes for sodium ion batteries.

Going forward additional steps can be taken to ensure a successful polymerization. For example, the anthraquinone can be dissolved into anhydrous toluene and left to evaporate. This followed by drying in a vacuum oven should give completely dry powder suitable for polymerization. As for NTCDA simply focusing on getting the pH values right and worrying less about the numerical quantities would likely give a much faster and higher yield synthesis. Then going into the polymerization an excess of dichloromethane could be used, as it is supposed to dissolve in this solvent. However, if that still fails the end to end polymerization of PNTCDA used NMP as the solvent so that could be used as the solvent instead.

It is worth noting that polymerization may not be the best way to achieve the desired result of reducing the solubility of organic materials in electrolytes. The ironic difficulty in making these materials is that functionalizing them with the tails necessary for polymerization already decreases solubility, although the materials should be highly soluble in order to make polymers, which in turn are not soluble [2]. Another possible option could be to research coatings for the electrodes which render the material insoluble or simply find alternative compounds [46].

6.2 Materials

No matter how much effort is put into choosing and making a material it is never a guarantee that it works. Being able to witness good performance of certain electrodes in half cells and then make some successful full cells was rewarding, but as these tests used monomers opposed to polymers most of the results were not very shocking. The ND solubility problems were expected and with naphthalimide the functional tail made the experiment an inaccurate representation of the performance if the desired polymer material were tested. However, the success of monomer ND in aqueous electrolyte indicated that polymerization may not be necessary as it was insoluble in water. Until the polymer NTCDA is tested it cannot be said whether or not this materials offers any advantage over ND. Therefore, it only reasonable to suggest other materials that may achieve the same result and potentially with a lot less effort.

a. 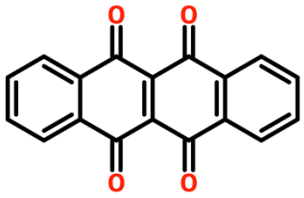 b. 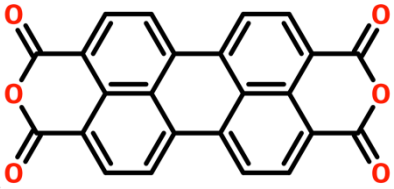

Figure x: a. Dioxotetracene quinone (similar to anthraquinone) b. Perylene Dianhydride

In trying to find materials with functionalizations that either reduced solubility or added capacity an old organic molecule was re-discovered called dioxotetracene quinone. It is very similar to anthraquinone, except with an extra benzene ring and two extra oxygens. Several papers were written about this molecule in the early 1900s by some German researchers, but it may be worthwhile to re-investigate this material as the extra oxygen atoms will provide additional bonding sites for sodium and the larger molecule may even reduce solubility eliminating the need for polymerization [4]. Another version of this material exists with an extra benzene ring in the middle and would likely prove to be even less soluble [2][43]. Given the hassle of digging up 100 year old papers and translating them from German, a more realistic idea would be to test perylenes.

Standard and readily available perylene dianhydride has been used as a successful anode versus sodium and lithium. It's redox plateaus also occur at slightly higher voltages versus Na than the anodes used in this project, so that would further ensure that the cell potential stays within the stability window of water. It it shown to work as pure compound, but can also be polymerized and functionalized should certain attributes be needed [5][36]. Admittedly, upon discovering this a last minute attempt was made to create coatings and do some preliminary cell cycling. Not enough time was spent on this to say anything conclusive or put in the results section.

6.3 Testing

Once the materials are chosen and made there is not much one can do to make them work in a cell. One can adjust the voltage and current settings as well as make changes to the coating process, but if a material fails to work for a fundamental reason then it is only possible to identify why and try to adjust accordingly. Due to the difficulty in going to a proven organic cell to an aqueous one, it might also be worthwhile to investigate the H_2O/electrode interface interactions. This could be done by adapting the current aqueous setup to take a sodium permeable membrane between the electrodes as to allow for one side to contain organic electrolyte while the other contains aqueous electrolyte. This would facilitate aqueous half cell testing which can normally not be done due to the reaction between water and sodium. Additionally, this might provide the missing piece of the puzzle as we would be able to see the the individual performance of the material against sodium in water. This may give insights as to what causes the large overpotentials seen in the aqueous test. Considering the success of the aqueous full cells, it seems clear that with more insight into the electrochemical mechanisms in water it will be possible to identify and mitigate the issues at hand.

Acknowledgements

I cannot complete this report without thanking all the people who have helped in many various ways. Firstly, I would like to thank my parents for their continued support during my time abroad. Ms. West I also missed you greatly and can't wait to get home and see you! Having never done organic chemistry before, I am grateful to Wolter for his tremendous help in making these polymers, let alone working with someone as ill-prepared to be in the lab as I was. Remco, thank you for everything, from explaining to me how to use the Maccor to interpreting results or trying to keep me optimistic when all the organic syntheses were going badly. Also, the living legend of the RID, Frans, has been incredibly pivotal in offering insights that became instrumental in my research, so I deeply thank you for your kind support. Lastly, there is one very interesting character I would like to thank; Santhosh Shetty. We've been through it all, everything from Ceramics to radiation life to algo crypto trading; it's been real!
#cryptoretirement

SFDBLB

Bibliography

1 Bhosale, Sheshanath V., Chintan H. Jani, and Steven J. Langford. "Chemistry of naphthalene diimides." *Chemical Society Reviews* 37.2 (2008): 331-342.

2 Buckton, Graham, and Anthony E. Beezer. "The relationship between particle size and solubility." *International journal of pharmaceutics* 82.3 (1992): R7-R10.

3 Chen, Long, et al. "Polyimide as anode electrode material for rechargeable sodium batteries." *RSC Advances* 4.48 (2014): 25369-25373.

4 Deichler, Chr, and Ch Weizmann. "Studien und Synthesen in der Reihe des Naphtacenchinons." *European Journal of Inorganic Chemistry* 36.1 (1903): 547-560.

5 Deng, Wenwen, et al. "A perylene diimide crystal with high capacity and stable cyclability for Na-ion batteries." *ACS applied materials & interfaces* 7.38 (2015): 21095-21099.

6 Devaraj, S., and N. Munichandraiah. "Effect of crystallographic structure of MnO2 on its electrochemical capacitance properties." *The Journal of Physical Chemistry C* 112.11 (2008): 4406-4417.

7 Doeff, Marca M., et al. "Orthorhombic Na x MnO2 as a Cathode Material for Secondary Sodium and Lithium Polymer Batteries." *Journal of the Electrochemical Society* 141.11 (1994): L145-L147.

8 EIA. "Hydroelectric Pumped Storage Electricity Installed Capacity." eia.gov (2018)

9 Engelke, Simon. "Current and future sodium-ion battery research." *International Journal of Energy Storage.–Draft* (2013): 1-7.

10 EPRI. "Electricity Energy Storage Technology Options: A White Paper Primer on Applications, Costs and Benefits." *Report* (2010).

11 Greenpeace, E. P. I. A. "Solar generation 6. Solar photovoltaic electricity empowering the world." *European Photovoltaic Industry Association, Greenpeace Report. Source: http://www. google. com/url* (2011).

12 Gottlieb, Hugo E., Vadim Kotlyar, and Abraham Nudelman. "NMR chemical shifts of common laboratory solvents as trace impurities." *The Journal of organic chemistry* 62.21 (1997): 7512-7515.

13 Guo, Chunyang, et al. "High-performance sodium batteries with the 9, 10-anthraquinone/CMK-3 cathode and an ether-based electrolyte." *Chemical Communications* 51.50 (2015): 10244-10247.

14 Hasa, Ivana, et al. "A sodium-ion battery exploiting layered oxide cathode, graphite anode and glyme-based electrolyte." *Journal of Power Sources* 310 (2016): 26-31.

15 Haxel, Gordon B., et al. *Rare earth elements: critical resources for high technology*. No. 087-02. 2002.

16 Hunter, James C. "Preparation of a new crystal form of manganese dioxide: λ-MnO2." *Journal of Solid State Chemistry* 39.2 (1981): 142-147.

17 Iordache, Adriana, et al. "Monothioanthraquinone as an organic active material for greener lithium batteries." *Journal of Power Sources* 267 (2014): 553-559.

18 Jung, Young Hwa, et al. "Na 2 FeP 2 O 7 as a positive electrode material for rechargeable aqueous sodium-ion batteries." *Rsc Advances* 4.19 (2014): 9799-9802.

19 Kielland, Knut. "Short-circuiting the nitrogen cycle: ecophysiological strategies of nitrogen uptake in plants from marginal environments." *Plant Nutrient Acquisition*. Springer, Tokyo, 2001. 376-398.

20 Kim, Haegyeom, et al. "Aqueous rechargeable Li and Na ion batteries." *Chemical reviews* 114.23 (2014): 11788-11827.

21 Kitchaev, Daniil A., et al. "Thermodynamics of phase selection in MnO2 framework structures through alkali intercalation and hydration." *Journal of the American Chemical Society* 139.7 (2017): 2672-2681.

22 Kundu, Dipan, et al. "The emerging chemistry of sodium ion batteries for electrochemical energy storage." *Angewandte Chemie International Edition* 54.11 (2015): 3431-3448.

23 Le, Thao P., Joy E. Rogers, and Lisa A. Kelly. "Photoinduced electron transfer in covalently linked 1, 8-naphthalimide/viologen systems." *The Journal of Physical Chemistry A* 104.29 (2000): 6778-6785.

24 Li, Jing, et al. "Asymmetric Supercapacitors with High Energy and Power Density Fabricated Using LiMn2O4 Nano-rods and Activated Carbon Electrodes." *INTERNATIONAL JOURNAL OF ELECTROCHEMICAL SCIENCE* 12.2 (2017): 1157-1166.

25 Liu, Bo, et al. "Converting cobalt oxide subunits in cobalt metal-organic framework into agglomerated Co3O4 nanoparticles as an electrode material for lithium ion battery." *Journal of Power Sources* 195.3 (2010): 857-861.

26 Lutgens, Frederick K., Edward J. Tarbuck, and Dennis Tasa. *Essentials of geology*. Vol. 480. Upper Saddle River, NJ: Prentice Hall, 2000.

27 Matsunaga, Yuki, et al. "Photoinduced color change and photomechanical effect of naphthalene diimides bearing alkylamine moieties in the solid state." *Chemistry-A European Journal* 20.24 (2014): 7309-7316.

28 Nayak, P. K., et al. "From Lithium-Ion to Sodium-Ion Batteries: Advantages, Challenges, and Surprises." *Angewandte Chemie (International ed. in English)* (2017).

29 Oltean, Viorica-Alina, et al. "Sustainable materials for sustainable energy storage: organic Na electrodes." *Materials* 9.3 (2016): 142.

30 Parant, Jean-Paul, et al. "Sur quelques nouvelles phases de formule NaxMnO2 (x⩽1)." *Journal of Solid State Chemistry* 3.1 (1971): 1-11.

31 Pasta, Mauro, et al. "A high-rate and long cycle life aqueous electrolyte battery for grid-scale energy storage." *Nature communications* 3 (2012): 1149.

32 E-education.psu.edu. Pennsylvania State University. "*Basic Polymer Structure | MATSE 081: Materials In Today's World"*. Available at: https://www.e-education.psu.edu/matse81/node/2210 [Accessed 21 Jun. 2018]

33 Qu, Q. T., et al. "A new cheap asymmetric aqueous supercapacitor: Activated carbon//NaMnO2." *Journal of Power Sources* 194.2 (2009): 1222-1225.

34 Ren, Yi, et al. "Pressure-Induced Neutral-to-Ionic Transition in an Amorphous Organic Material." *Chemistry of Materials* 28.18 (2016): 6446-6449.

35 Sassi, Mauro, et al. "Gray to Colorless Switching, Crosslinked Electrochromic Polymers with Outstanding Stability and Transmissivity From Naphthalenediimmide-Functionalized EDOT." *Advanced Materials* 24.15 (2012): 2004-2008.

36 Sharma, Pavan, et al. "Perylene-polyimide-Based organic electrode materials for rechargeable lithium batteries." *The Journal of Physical Chemistry Letters* 4.19 (2013): 3192-3197.

37 Speight, James G. *Lange's handbook of chemistry*. Vol. 1. New York: McGraw-Hill, 2005.

38 Tarascon, J. M., et al. "Chemical and electrochemical insertion of Na into the spinel λ-MnO2 phase." *Solid State Ionics* 57.1-2 (1992): 113-120.

39 Tarascon, J-M., and Michel Armand. "Issues and challenges facing rechargeable lithium batteries." *Materials For Sustainable Energy: A Collection of Peer-Reviewed Research and Review Articles from Nature Publishing Group*. (2011). 171-179.

40 Tevar, A. D., and J. F. Whitacre. "Relating synthesis conditions and electrochemical performance for the sodium intercalation compound Na4Mn9O18 in aqueous electrolyte." *Journal of The Electrochemical Society* 157.7 (2010): A870-A875.

41 Vadehra, Geeta S., et al. "Naphthalene diimide based materials with adjustable redox potentials: evaluation for organic lithium-ion batteries." *Chemistry of Materials* 26.24 (2014): 7151-7157.

42 Van Noorden, Richard. "A better battery." *Nature* 507.7490 (2014): 26.

43 Vets, Nathalie, et al. "Synthesis of 5, 7, 12, 14-tetraarylpentacenes from pentacene-5, 7, 12, 14-tetrone and characterisation of the tetrol intermediates." *Synlett* 2006.09 (2006): 1359-1362.

44 Wan, Wang, et al. "Tuning the electrochemical performances of anthraquinone organic cathode materials for Li-ion batteries through the sulfonic sodium functional group." *RSC Advances* 4.38 (2014): 19878-19882.

45 Wang, Heng-guo, et al. "Tailored Aromatic Carbonyl Derivative Polyimides for High-Power and Long-Cycle Sodium-Organic Batteries." *Advanced Energy Materials* 4.7 (2014).

46 Wang, Xujiong, et al. "An aqueous rechargeable lithium battery using coated Li metal as anode." *Scientific reports* 3 (2013): 1401.

47 Whitacre, J. F., et al. "An aqueous electrolyte, sodium ion functional, large format energy storage device for stationary applications." *Journal of Power Sources* 213 (2012): 255-264.

48 Whitacre, J. F., A. Tevar, and S. Sharma. "Na4Mn9O18 as a positive electrode material for an aqueous electrolyte sodium-ion energy storage device." *Electrochemistry Communications* 12.3 (2010): 463-466.

49 World Watch Institute. "Short-circuiting the Global Phosphorus Cycle." www.worldwatch.org/node/516. Published in World Watch Magazine March/April 2002, Volume 15, No. 2.

50 Yabuuchi, Naoaki, et al. " Electrochemical behavior and structural change of spinel-type Li [LixMn2− x] O4 (x= 0 and 0.2) in sodium cells." *Electrochimica Acta* 82 (2012): 296-301.

51 Yang, Dong-Hui, et al. "Structure-modulated crystalline covalent organic frameworks as high-rate cathodes for Li-ion batteries." *Journal of Materials Chemistry A* 4.47 (2016): 18621-18627.

52 Yang, Shun-Yi, et al. "Effects of Na content on structure and electrochemical performances of NaxMnO2+ δ cathode material." *Transactions of Nonferrous Metals Society of China* 20.10 (2010): 1892-1898.

53 Yao, Masaru, et al. "Crystalline polycyclic quinone derivatives as organic positive-electrode materials for use in rechargeable lithium batteries." *Materials Science and Engineering: B* 177.6 (2012): 483-487.

54 Zeng, Juqin, et al. "Li-O 2 cells based on hierarchically structured porous alpha-MnO2 catalyst and an imidazolium based ionic liquid electrolyte." *Int J Electrochem Sci* 8.3 (2013): 3912-3927.

55 Zhang, Ying, et al. "An aqueous capacitor battery hybrid device based on Na-ion insertion-deinsertion in λ-MnO2 positive electrode." *Electrochimica Acta* 148 (2014): 237-243.

56 Zhao, Kang, et al. "Enhanced efficiency of polymer photovoltaic cells via the incorporation of a water-soluble naphthalene diimide derivative as a cathode interlayer." *Journal of Materials Chemistry C* 3.37 (2015): 9565-9571.

Appendix

H_2 and O_2 Evolution Derivations

The hydrogen evolution reaction can be written as below:

$$2H^+ + 2e^- \rightleftharpoons H_2 \qquad \text{(Eq. 1)}$$

The equilibrium constant for this reaction is:

$$K = \frac{P_{H_2}/P_0}{[H^+]^2} \qquad \text{(Eq. 2)}$$

Where P_{H_2} is the pressure of hydrogen gas at 1 bar, P_0 is standard atmospheric pressure 1.01 bar, and H^+ is the concentration of hydrogen ions. Equation 2 will be needed to plug into the Nernst Equation below:

$$E = E_0 - \frac{RT}{nF}\ln(K) \text{(Eq. 3)}$$

Where E is the voltage, E_0 is the standard half cell potential in volts, R is the gas constant (8.314 J/(mol*K)), T is temperature in Kelvin, n is the number of electrons transferred, and F is the Faraday constant (96485 C/mol). Before substitution is is easier to rewrite Equation 3 ad 4 in logarithmic form. The definition of pH is also in logarithmic form and will needed.

$$\log(K) = \log\left(P_{H_2}\right) - 2\log([H^+]) \qquad \text{(Eq. 4)}$$

$$E = E_0 - \frac{2.303RT}{nF}\log(K) \qquad \text{(Eq. 5)}$$

$$pH = -\log([H^+]) \qquad \text{(Eq. 6)}$$

Now substituting Equation 4 into Equation 5 leads to:

$$E_{H_2} = E_{H^+/H_2} - \frac{2.303RT}{nF}\left(\log\left(P_{H_2}\right) - 2\log([H^+])\right) \qquad \text{(Eq. 7)}$$

Knowing the half cell potential of hydrogen (H^+/H_2) is -0.21 V, assuming the the pressure of hydrogen is 1 bar, and using the definition of pH the equation can begin to be simplified.

$$E_{H_2} = E_{H^+/H_2} + \frac{2.303RT}{nF}2\,pH \qquad \text{(Eq. 8)}$$

Lastly, all the variables can be plugged in, which are T=297 Kelvin and n=2 electrons transferred. This gives the final equation relating the hydrogen evolution potential as a function of pH:

$$E_{H_2} = -0.21 - 0.0592\,pH \qquad \text{(Eq. 9)}$$

The derivation of the O_2 evolution can be done in a very similar fashion beginning with oxygen evolution reaction and corresponding equilibrium constant:

$$O_2 + 4H^+ + 4e^- \rightleftharpoons 2H_2O \quad \text{(Eq. 10)}$$

$$K = \frac{[H_2O]^2}{[O_2][H^+]^4} = \frac{1}{[\frac{P_{O_2}}{P_0}][H^+]^4} \quad \text{(Eq. 11)}$$

The same logarithmic conversion can be done again for the equilibrium constant giving:

$$\log(K) = -\log(P_{O_2}) - 4\log([H^+]) \quad \text{(Eq. 12)}$$

Following the same steps as for the hydrogen evolution derivation, we can easily arrive at the following:

$$E_{O_2} = E_{O_2/H_2O} - \frac{2.303RT}{nF}4pH \quad \text{(Eq. 13)}$$

Knowing the standard half cell potential for oxygen is 1.019 volts and the number of transferred is 4 we can then plug in the same constants and variables as before to yield:

$$E_{O_2} = 1.019 - 0.0592\ pH \quad \text{(Eq. 14)}$$

XRD Peak Spectra

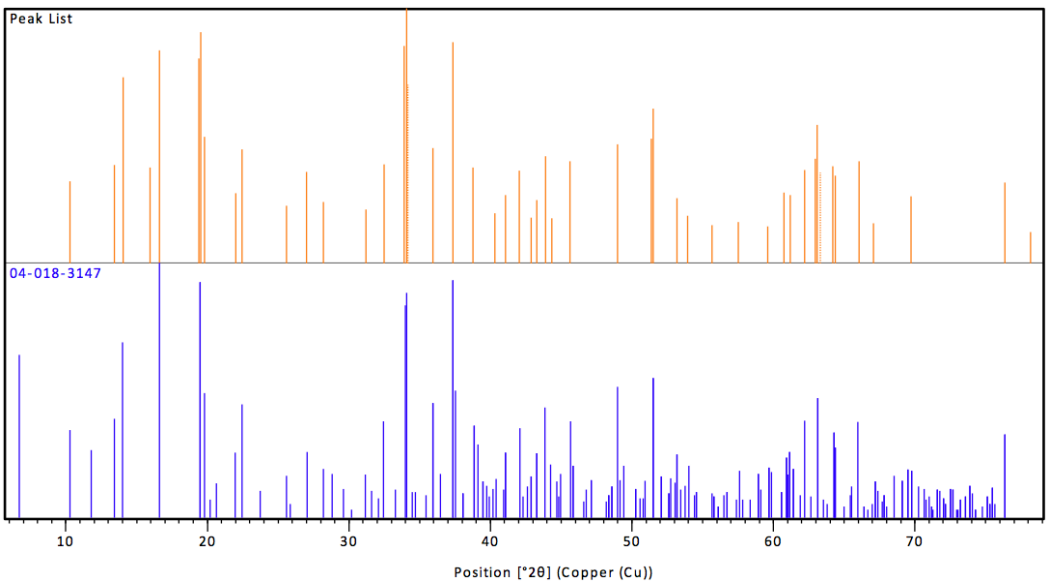

Figure 1: $Na_{0.44}MnO_2$ Peak list compared to Joint Committee on Powder Diffraction Standards (JCPDS) database spectrum

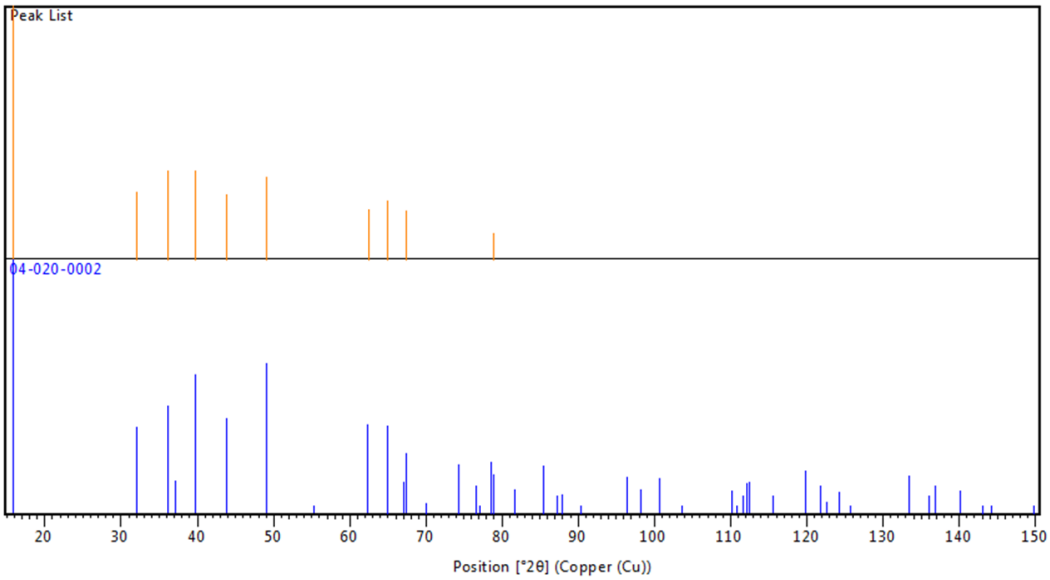

Figure 2: $Na_{0.66}MnO_2$ Peak list compared to JCPDS database spectrum

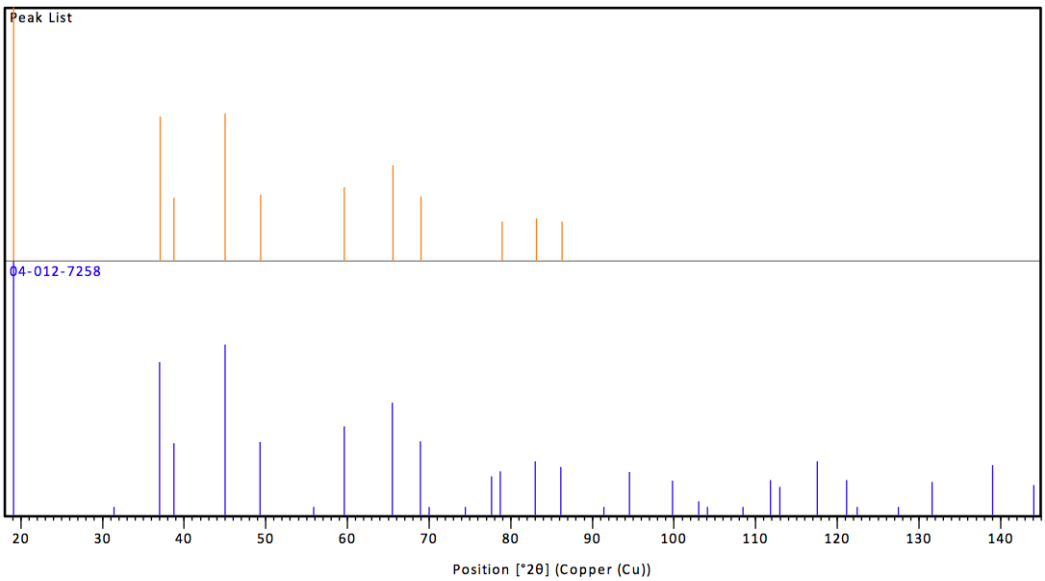

Figure 3: λ-MnO_2 Peak list compared to JCPDS database spectrum

NMR Spectra

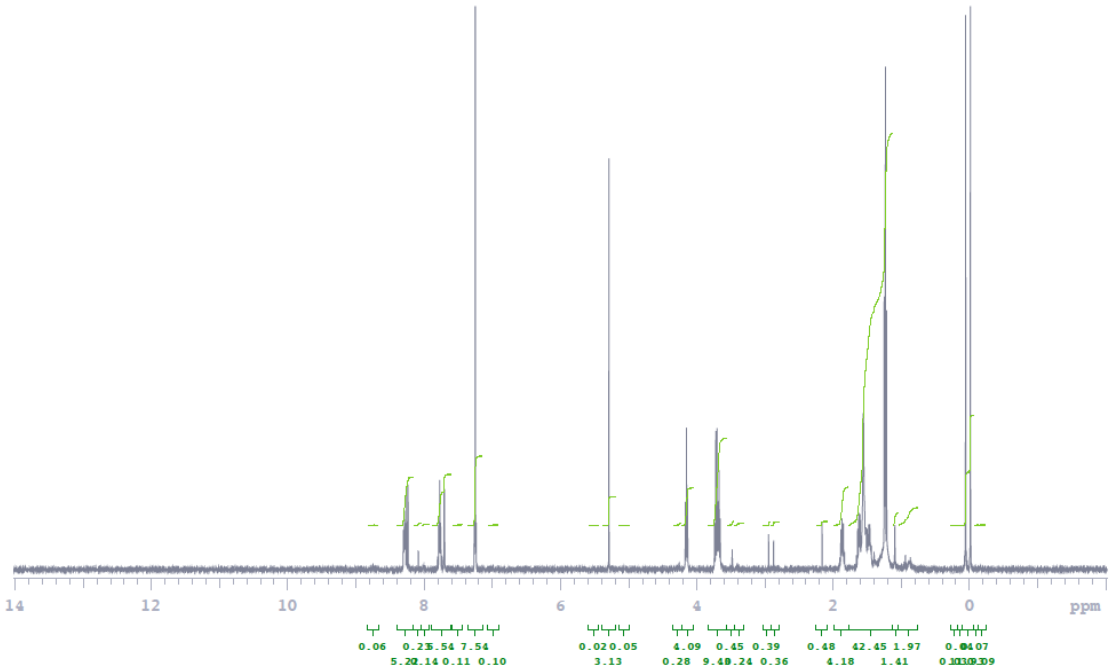

Figure 4: Anthraquinone with impurities NMR spectrum

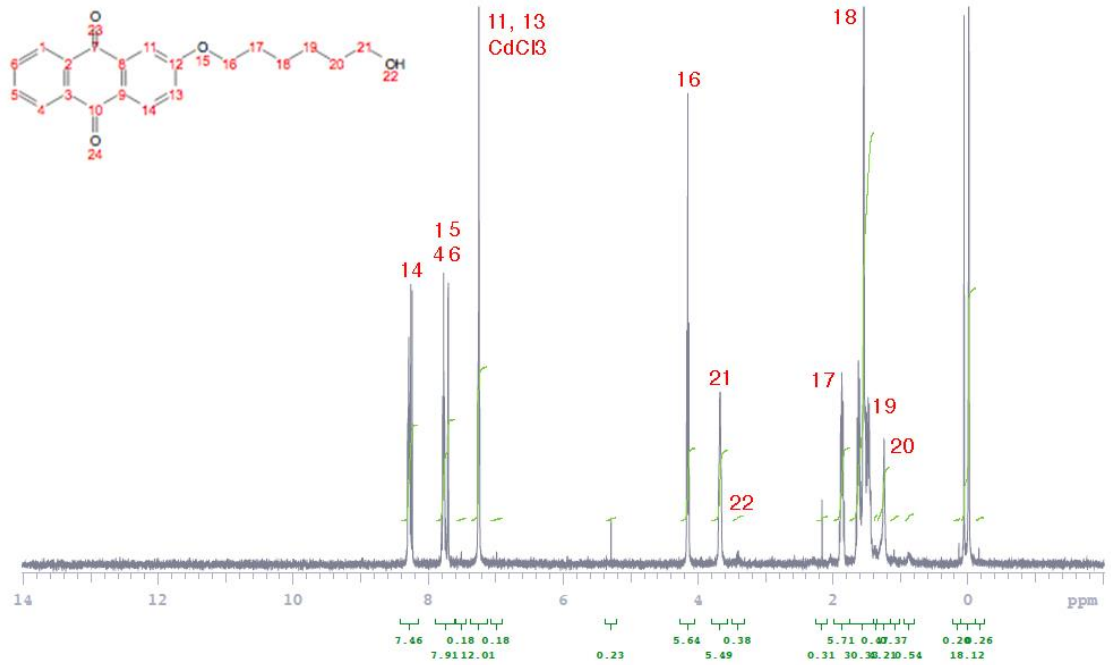

Figure 5: Pure anthraquinone after column chromatography NMR spectrum

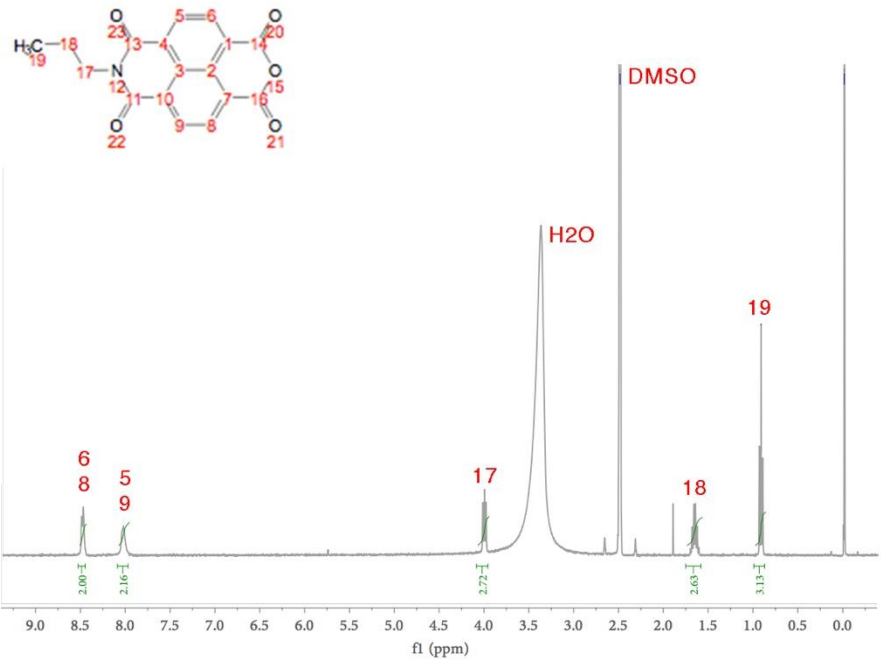

Figure 6: NTCDA after first synthesis step NMR spectrum

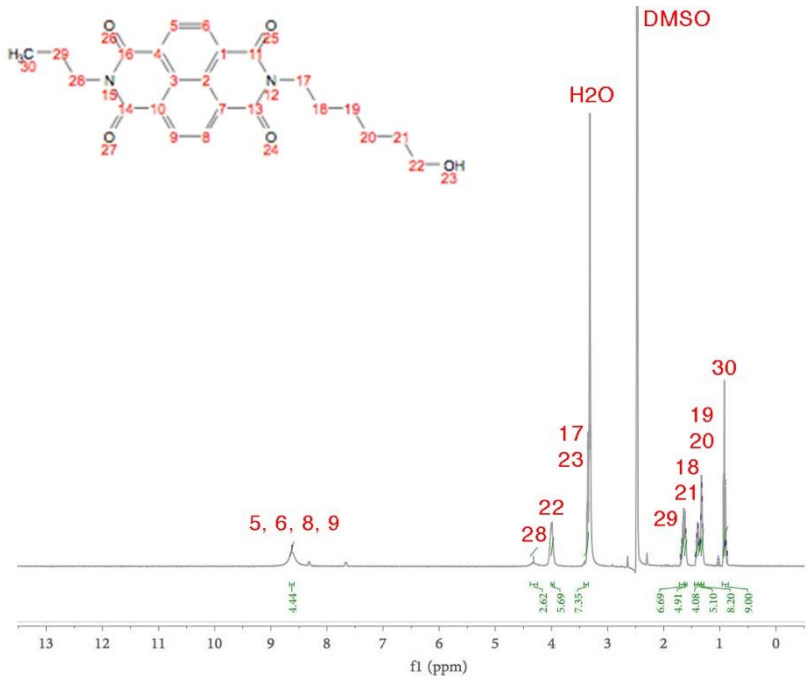

Figure 7: Pure NTCDA after recrystallization NMR spectrum

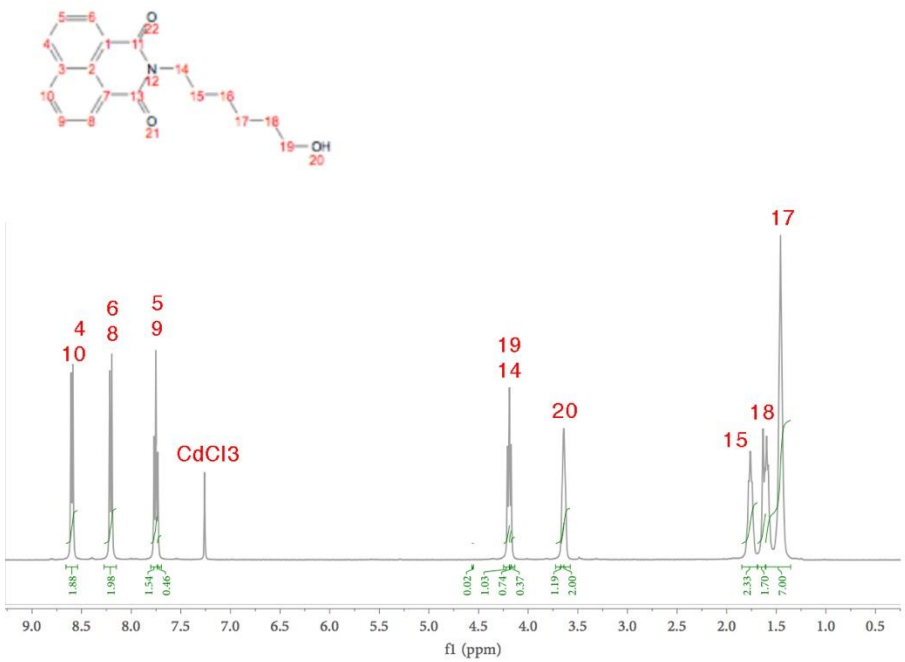

Figure 8: Naphthalimide NMR spectrum

Additional Cell Tests

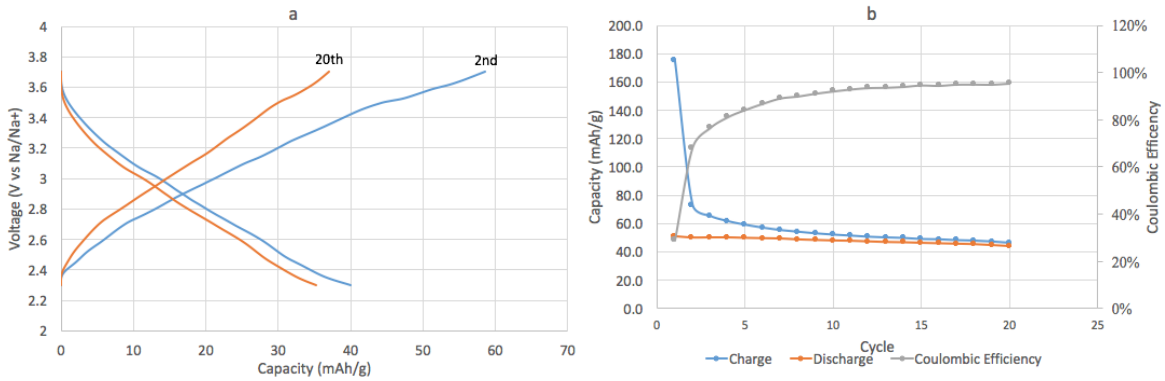

Figure 9: a. (Dis)Charge Curves and b. Cycle Chart for $Na_{0.66}MnO_2$ at 0.1C

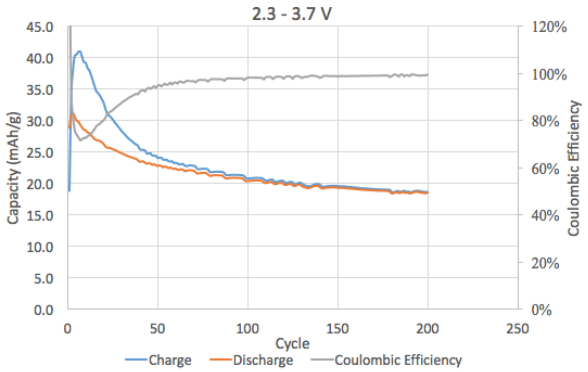

Figure 10: Cycle Chart for $Na_{0.66}MnO_2$ at 1C Rate

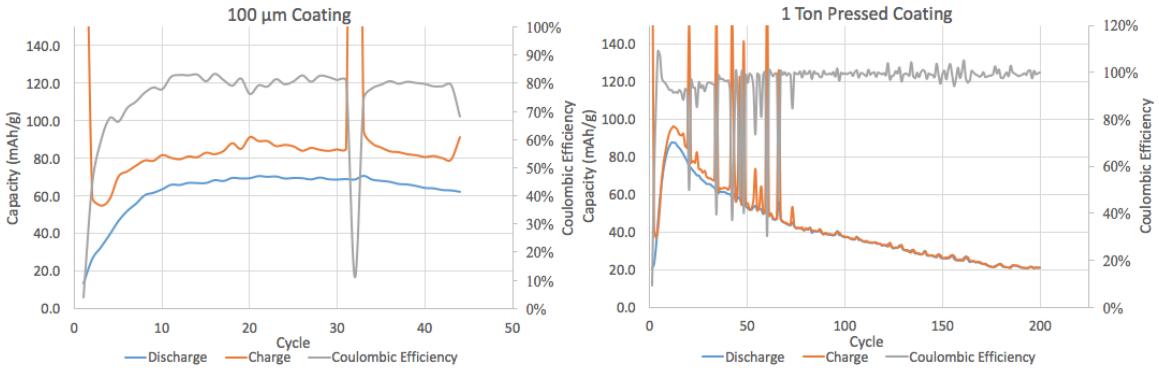

Figure 9: λ-MnO_2 Test with alternative coatings at C/10 Rate